CHALMERS

Group Delay Variations in Microwave Filters and Equalization Methodologies

Master 's Thesis in Microtechnology and Nanoscience

YU SU

Department of Microtechnology and Nanoscience (MC2)

CHALMERS UNIVERSITY OF TECHNOLOGY, Göteborg

Microwave and High Speed Electronics Research Center

Ericsson research, ERICSSON AB, Mölndal

Sweden, 2012

Group Delay Variations in Microwave Filters and Equalization Methodologies

YU SU

Department of Microtechnology and Nanoscience (MC2)

Chalmers University of Technology

Microwave and High Speed Electronics Research Center

Ericsson AB

Sweden, 2012

Group Delay Variations in Microwave Filters and Equalization Methodologies

YU SU

Department of Microtechnology and Nanoscience (MC2)

Chalmers University of Technology

SE-412 96 Göteborg, Sweden

Microwave and High Speed Electronics Research Center

Ericsson AB

SE-431 84 Mölndal, Sweden

Abstract

In modern telecommunication systems, a constant group delay is necessary in order to avoid signal distortion. Unfortunately, a group delay variation is unavoidable. For example, a band-pass filter in microwave systems will create a group delay variation near the edge of pass band, i.e., in transition areas of the filter. According to simulations of ideal filter components (Q is infinite) in ADS, it shows a 5th-order Elliptic band-pass filter with stopband rejection of 20 dB and pass-band frequency from 7.5 GHz to 12.5 GHz would introduce a maximum group delay variation of 3.4 ns. System simulations in *MATLAB* show that it would cost extra power of 0.8 dB and 1.6 dB for 4QAM and 16QAM modulation respectively, to achieve the same performance (bit-error-rate) as the system without any group delay variation. Therefore, it is necessary to develop so-called group delay equalizers to compensate the variation of the group delay.

Analog group delay equalizers are realized based on two methodologies: 1) all-pass networks, which are used to generate a positive group delay with desired features; 2) a negative group delay circuit, which is used to compensate group delay variation originating from filters. Unfortunately, the existing negative group delay circuit suffers from a large attenuation in the frequency range where negative group delay occurs. In this thesis, a novel group delay equalizer circuit topology is proposed, to overcome the drawback of large attenuation. It is demonstrated that the proposed negative group delay circuit has a flat amplitude response with a variation less than 0.6 dB, keeping a feature of negative group delay. As example, the proposed equalizer is used to compensate the group delay variation originating from a low-pass filter with the pass-band from DC to 15 GHz. The simulation result exhibits that the group delay variation of the filter is reduced from 0.6 ns to 0.2 ns while the amplitude response is reduced less than 0.53 dB due to losses of the equalizer. For band-pass filters, one more stage of the proposed equalizer is needed in order to compensate the group delay variation in both sides of filters.

Keywords: Group delay variation, group delay equalization, all-pass network, negative group delay, band-pass filter.

Acknowledgements

First of all, I would like to express my gratitude to my supervisor Mingquan Bao. Thanks for constant help, support, and never ceasing ideas. I would also like to thank my supervisor and examiner in Chalmers Dan Kuylenstierna. Thank you for discussions and proof reading my thesis.

I am very grateful to everyone in the Ericsson Research group for help and interesting discussions and special thanks to my co-supervisor Anna Rhodin for computer support and the administration.

Finally, I would like to thank to my friends and family. Thanks for your help and support.

Abbreviations

AD	Analog-to-digital
ADS	Advance Design System
ANGD	Active Negative Group Delay
APN	All-pass Network
AWGN	Additive White Gaussian Noise
BER	Bit Error Rate
CAD	Computer Aided Design
CD	Chromatic Dispersion
CRLH	Composite Right and Left Hand
DA	Digital-to-analog
DDL	Dispersive Delay Line
DSP	Digital Signal Processing
FIR	Finite Impulse Response
GDV	Group Delay Variation
IIR	Infinite Impulse Response
ISI	Inter-symbol Interference
MIC	Microwave Integrated Circuit
MMIC	Monolithic Microwave Integrated Circuit
MSW	Magneto-Static Wave
NGD	Negative Group Delay
PCB	Printed Circuit Board
PHEMT	Pseudomorphic High Electron Mobility Transistor
Q	Quality Factor
QAM	Quadrature Amplitude Modulation
QPSK	Quadrature Phase Shift Keying
RNGD	Reflection-type Negative Group Delay
SAW	Surface Acoustic Wave
SNR	Signal-to-noise Ratio
SPR	Series-parallel Resonance

SSR	Shunt-series Resonance
UWB	Ultra-wide Band
ZF	Zero-forcing

Table of Contents

Chapter 1

Introduction

In high speed telecommunication systems, undesired dispersion effects are problematic and could degrade overall system performance. The group delay variation would distort the waveform of signals, resulting in the inter-symbol interference (ISI), which introduces errors in communication systems.

In optical communications, compensating for the group delay variation, also called chromatic dispersion (CD), has been one of the main challenges in the design of optical transceivers. The reason causing the group delay variation in standard fibers is that different spectral components of the transmitted optical signal travel at different velocities, resulting in different time delay to reach the end of fibers. A group delay variation might severely distort the optical waveform which contains information and even cause the failure of whole systems. Similarly, in microwave communications, some microwave devices may cause group delay variations, such as amplifiers, filters and mixers. For ultra-wide band (UWB) applications [1], the data information is based on impulse signals; in the presence of group delay variation, received impulse signals might be reshaped and fatal error occurs. As a consequence, equalization for group delay variation becomes indispensible.

To compensate the effect of group delay variation in systems, digital techniques based on infinite impulse response (IIR) filters or finite impulse response (FIR) filters are widely used in digital signal processing (DSP) domain [2]. Normally digital devices are attractive due to their high flexibility and reliability, but they are limited by the performance of analog-to-digital (AD) / digital-to-analog (DA) converters which generally suffer from excessive cost as well as large power consumption for high speed applications [3].

Instead, the analog equalization could be a good alternative to deal with the group delay variation. An equalizer based on analog all-pass filters, which has a flat amplitude response and group delay response with a specified characteristic, has been developed since 1970s [4] [5]. During recent years, dispersive delay lines (DDLs) has become a hot topic not only for analog signal processing but also for group delay compensation [6]. Several DDL solutions have been proposed and

investigated, e.g., utilizing surface acoustic wave (SAW) [7] and magneto-static wave (MSW) [8]. A SAW DDL presents some advantages such as compact size but it is limited to operation at low frequency (< 2 GHz), while a MSW DDL can operate at high frequency but suffers from complex fabrication and high loss [9]. The chirped delay line is also a good solution. A good performance can be achieved, but it usually consumes a large substrate size [10] [11] [12]. In addition, composite right and left hand (CRLH) techniques [13] are also used to construct the DDL and several applications have been proposed [6] [14] [15]. The analog equalizers mentioned above would generate a positive group delay with desired features. In contrast, negative group delay (NGD) circuits have opened up prospects for group delay compensation [16], which could compensate the group delay variation without increasing total group delay time [17] [18] [19]. However, it suffers from a large attenuation within the frequency range where the negative group delay occurs.

The effect of group delay variation is difficult to calculate analytically for complex modulations in practical communication systems, but relatively simple by simulation with the help of *MATLAB* software. In this thesis, the effect of group delay variation from band-pass filters for 4QAM and 16QAM modulation will be simulated and evaluated based on the bit error rate. In the simulations, group delay variation is added in the receiver front end, while other components in the transceiver are assumed to be perfect. Furthermore, group delay equalization for filters will be investigated and discussed. Some methodologies based on microwave circuits will be presented, as well as the corresponding simulation results in *Agilent Advance Design System* (ADS) software. Eventually, a novel group delay equalization method is proposed, which is based on reflection-type negative group delay circuits with negative resistance.

The thesis is organized as follows. In Chapter 2 background knowledge about the definition of group delay as well as group delay equalization is presented. Chapter 3 is dedicated to evaluate the effect of the group delay variation on communication systems by both theoretical analysis and simulations. The simulations are focused on the effect of group delay variation from band-pass filters and the results are presented in terms of the bit error rate and penalty power. Chapter 4 is concerned with several methodologies for group delay equalization based on microwave circuits. The chapter starts with all-pass networks, followed by negative group delay circuits. They are implemented by using lumped components and distributed transmission lines. Then, a novel group delay equalization method based on negative group delay circuits is proposed, which has a feature of a flat amplitude

response. Finally, conclusions of the thesis and the future work are presented in Chapter 5.

Chapter 2

Background

This chapter presents background knowledge that is related to this thesis. In Section 2.1, fundamental concepts of phase velocity, group velocity and group delay are presented. In Section 2.2, group delay variations in microwave components are investigated; while group delay equalization is introduced in Section 2.3.

2.1 Concepts

2.1.1 Phase velocity

A plane wave travelling along the z-direction can be expressed as

$$U(z,t) = Re\{U_0 e^{j(\omega t - kz)}\} \tag{2.1}$$

where U_0 is the peak amplitude; ω is the angular frequency and k is the wave number which is a function of ω.

Then, the phase velocity can be defined as

$$v_p = \frac{\omega}{k(\omega)} \tag{2.2}$$

For an electromagnetic wave travelling in the non-dispersive media, $k(\omega)$ is independent with the angular frequency; in this case, $k(\omega)$ is constant and the phase velocity is proportional to the angular frequency ω.

2.1.2 Group velocity

According to the Fourier theorem, any real electromagnetic signal can be expressed as a superposition of one or several single plane waves and each wave would travel with corresponding phase velocity $v_p(\omega)$. The entire signal can be written in an integral form as

$$\psi(z,t) = \frac{1}{\sqrt{2\pi}}\int_{-\infty}^{\infty} g(k)\, e^{j[\omega t - k(\omega)z]}dk\,, \tag{2.3}$$

where $g(k)$ is the Fourier transform of the signal at t = 0 :

$$g(k) = \frac{1}{\sqrt{2\pi}}\int_{-\infty}^{\infty} \psi(z,0)\, e^{jkz}dz \tag{2.4}$$

In order to understand the group velocity, let us consider a simple case with only two waves ($k_0 - \Delta k, \omega_0 - \Delta\omega$ and $k_0 + \Delta k, \omega_0 + \Delta\omega$), which is close to each other (i.e., $\Delta k \ll k_0$ and $\Delta\omega \ll \omega_0$) and has the same amplitude $g(k_0)$; thus, the group of waves is the summation of two single waves:

$$\psi(z,t) = \frac{1}{\sqrt{2\pi}} g(k_0)[e^{j(\omega_0 t - \Delta\omega t + k_0 z - \Delta k z)} + e^{j(\omega_0 t + \Delta\omega t + k_0 z + \Delta k z)}] \tag{2.5}$$

Using a trigonometric identity

$$\cos(\theta) = \frac{e^{j\theta}+e^{-j\theta}}{2}, \tag{2.6}$$

(2.5) can be rewrote as

$$\psi(z,t) = \frac{1}{\sqrt{2\pi}} g(k_0)[2\cos(\Delta\omega t - \Delta k z)e^{j(\omega_0 t - k_0 z)}] \tag{2.7}$$

From (2.7) it is clear to see that the term $2\cos(\Delta\omega t - \Delta k z)$ is the envelope of the signal and it would travel along the z-axis with a speed of

$$v_e = \frac{\Delta\omega}{\Delta k} \tag{2.8}$$

In the limit of $\Delta \to 0$, (2.8) can be expressed as

$$v_g = \frac{d\omega}{dk}\,, \tag{2.9}$$

which is the definition of the group delay velocity.

Since the information is only contained in the group of waves, the group velocity represents the speed of information propagation. For non-dispersive media, $k(\omega)$

is independent with ω, resulting in the constant of the group velocity. This means the signal having different frequencies would travel with the same speed. However, for dispersive media, the group velocity depends on the frequency, so that the information in different frequencies would travel with different speeds and the whole signal would be distorted. Normally a constant group velocity is a critical requirement for communication systems especially for data transmission based on impulses (e.g., UWB).

2.1.3 Group delay

For a wave travelling a certain distance L in a certain time τ, the velocity is defined by

$$v = \frac{L}{\tau} \tag{2.10}$$

Substituting the group velocity v_g into above equation, the group delay can be related as

$$\tau_g = \frac{L}{v_g} \tag{2.11}$$

However, for many electronic circuits, such as lumped components and amplifiers, the spatial extent or size of the device under study is negligible compared with the wavelength of the desired signal; thus, the concept of group delay has to be defined by the transfer function of a network $H(j\omega)$. The transfer function for a certain network can be expressed by a magnitude response $|H(j\omega)|$ and a phase response $\phi(\omega)$:

$$H(j\omega) = |H(j\omega)|e^{j\phi(\omega)} \tag{2.12}$$

Then, the group delay is given by the negative derivative of the phase response with the respect of the angular frequency as

$$\tau_g = -\frac{\partial\phi(\omega)}{\partial\omega} \tag{2.13}$$

In microwave circuits, the transfer function of a network can also be expressed as the scattering parameter (S-parameter) S_{21}; thus, the group delay can also be related by

$$\tau_g = -\frac{\partial \phi(S_{21})}{\partial \omega} \tag{2.14}$$

The definition of group delay in (2.14) will be used during the rest of this work, since most content would be discussed in microwave range.

2.2 Group delay in microwave components

In microwave communications, the group delay variation mainly originates from frequency-dependent devices, e.g. amplifiers, filters and mixers, where inductors and capacitors are widely used.

In order to analyze the phase response, let us rewrite the phase response as a Taylor series expansion around the centre frequency ω_0:

$$\begin{aligned}\phi(\omega) = \phi(\omega_0) + \left.\frac{d\phi}{d\omega}\right|_{\omega_0}(\omega-\omega_0) + \left.\frac{1}{2!}\frac{d^2\phi}{d\omega^2}\right|_{\omega_0}(\omega-\omega_0)^2 \\ + \left.\frac{1}{3!}\frac{d^3\phi}{d\omega^3}\right|_{\omega_0}(\omega-\omega_0)^3 + \cdots\end{aligned} \tag{2.15}$$

Then, the group delay can be obtained according to (2.13):

$$\tau_g = -\frac{\partial \phi(\omega)}{\partial \omega} = g_0 + g_1(\omega-\omega_0) + g_2(\omega-\omega_0)^2 + \cdots \tag{2.16}$$

where $g_0 = -\left.\frac{d\phi}{d\omega}\right|_{\omega=\omega_0}$, $g_1 = -\left.\frac{1}{1!}\frac{d^2\phi}{d\omega^2}\right|_{\omega=\omega_0}$, $g_2 = -\left.\frac{1}{2!}\frac{d^3\phi}{d\omega^3}\right|_{\omega=\omega_0}$ and high-order terms are omitted.

For systems with linear phase responses, only first term g_0 exists, which is constant and is called the zeroth-order group delay. For systems with non-linear phase responses, there are other terms: g_1 is the first-order group delay (linear group delay) and g_2 is the second-order group delay (parabolic group delay) as shown in Fig. 2. 1(a).

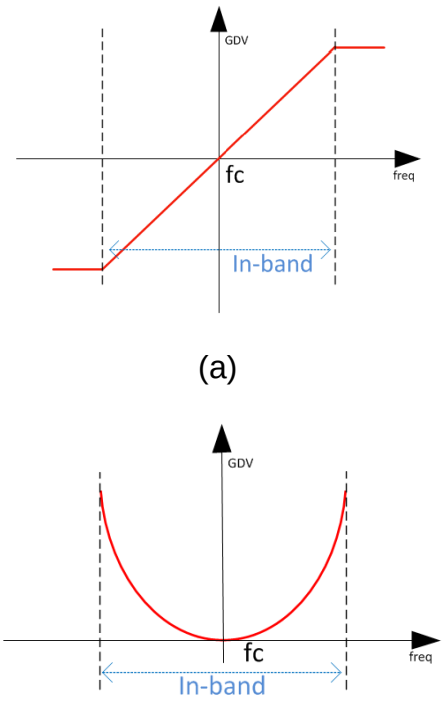

Fig. 2. 1: (a) The first-order and (b) second-order group delay variation

Typically, group delay variation (GDV) within the pass-band of microwave circuits is made up of the first-order (linear) and the second-order (parabolic) group delay, while the high-order group delay are negligible on account of slight affection to distortion.

The linear group delay is very general in optical communication, which is also called chromatic dispersion (CD) [20]. The reason for that is different spectral components of the transmitted optical signal would travel at different velocities in optical fibers, resulting in the group delay variation and normally it can be modeled as linear one. A typical group delay variation in standard single-mode fibers is shown in Fig. 2. 2. Recently, more and more optical fiber communications systems operate around 15-μm range due to lower losses. Thus, so-called dispersion-shifted fibers have been developed to shift the zero dispersion wavelength into the 1.5-μm region as shown in Fig. 2. 2 [21]. It also shows dispersion-flattened fibers which has a relatively constant group delay over some wavelength range.

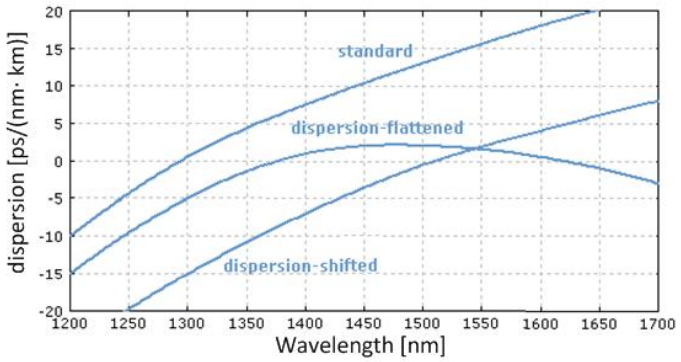

Fig. 2. 2: Group delay dispersion in standard, dispersion-shifted and dispersion-flattened single-mode fibers

In addition, the group delay variation in a band-pass filter contains the parabolic property as shown in Fig. 2. 3. The group delay characteristic depends on the type of filter; while for filters with same type, group delay increases as the order of a filter increases or as the bandwidth is reduced. The effect of filters with different types will be simulated and discussed further in chapter 3.

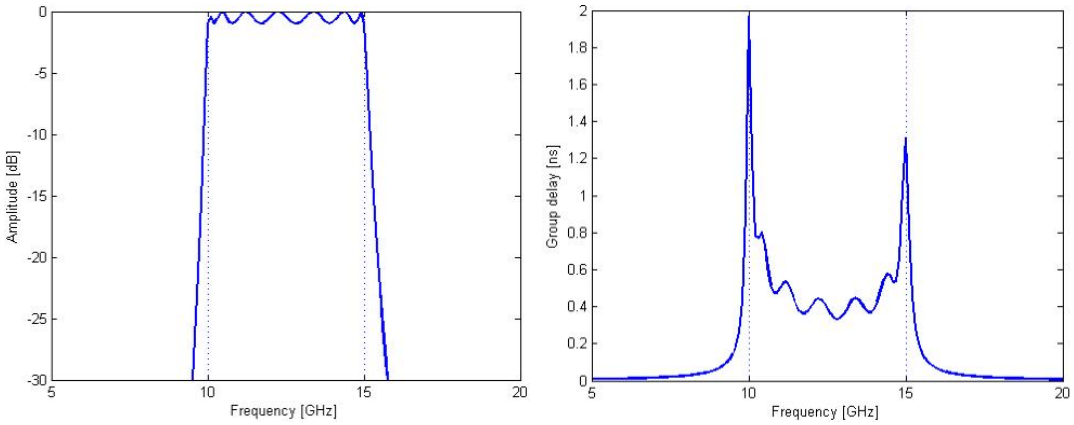

(a) (b)

Fig. 2. 3: (a) Amplitude response and (b) group delay of a Chebyshev filter with passband from 10GHz to 15GHz, stopband from 9.5GHz to 15.5GHz and stopband rejection of 20 dB (simulation results from the ideal filter components in ADS)

Similarly, for a low-pass filter, the group delay variation occurs near the edge of pass band, i.e., in transition areas of filters. The magnitude response and group delay performance of a typical low-pass filter are shown in Fig. 2. 4.

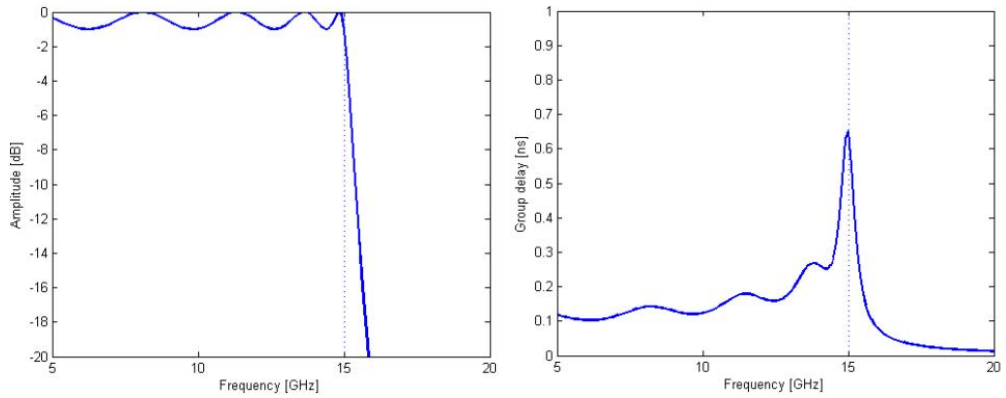

(a) (b)

Fig. 2. 4: (a) Amplitude response and (b) group delay of a Chebyshev low-pass filter with pass band from DC to 15Ghz (simulation results from the ideal filter components in ADS)

Another type of group delay variation is sinusoidal ripple, which is often caused by impedance mismatches in the system, such the discontinuity in the transmission line [22]. Normally it is also associated with amplitude ripple in the pass-band as shown in Fig. 2. 5. Since the GDV caused by reflection are sinusoidal with several cycles, it would be complicated to compensate them by GDV equalizers. However, it can be reduced or minimized by decreasing the dielectric constant, proper matching networks or well-placed attenuators, which reduce the power of reflection waves [23].

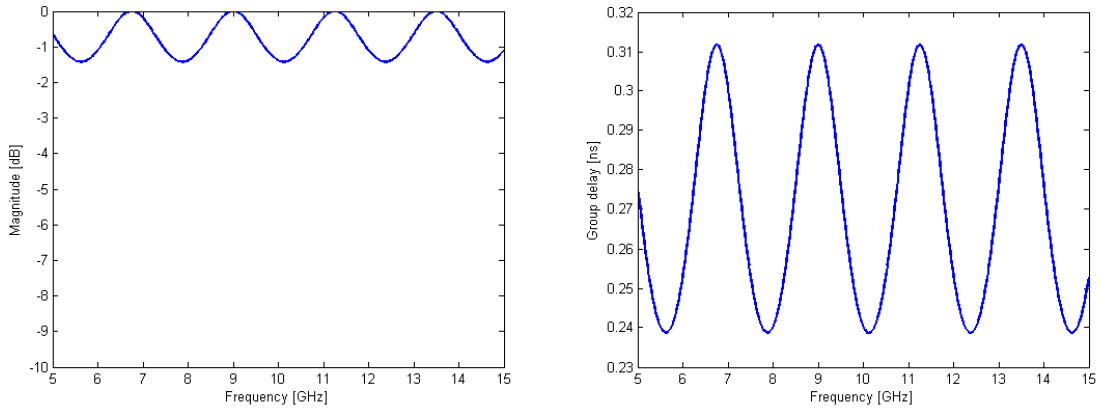

(a) (b)

Fig. 2. 5: (a) Magnitude response and (b) group delay of cascaded transmission lines with impedance mismatch (simulation results from the ideal transmission lines in ADS)

2.3 Group delay equalization

In communication systems, flat amplitude response and linear phase response (consistent group delay) are necessary in order to maintain the waveform of transmitted signals. Otherwise, the inter-symbol interference (ISI) would occur [24].

However, for most communication systems, the flat amplitude and linear phase response cannot be achieved due to impairments in the system, such as band-limited or frequency-selective properties; thus, the equalization is needed to compensate for those impairments in systems. In a broad sense, equalization defines any signal processing techniques used at the receiver or transmitter to alleviate the ISI problem caused by imperfect propertied of systems [25].

A simplest equalization is a zero-forcing (ZF) equalizer following the channel with non-linear phase response as shown in Fig. 2. 6.

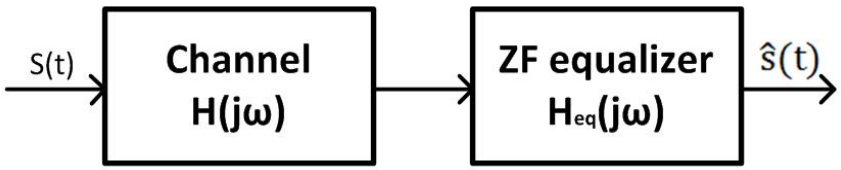

Fig. 2. 6: Block diagram of zero-forcing equalizer

The equalizer transfer function is inverse form of the channel:

$$H_{eq}(j\omega) = \frac{1}{H(j\omega)} = \frac{1}{|H(j\omega)|} e^{-j\phi(\omega)} \tag{2.17}$$

Thus, the original signal *s(t)* can be recovered at the output of the equalizer, i.e., $\hat{s}(t) = s(t)$.

In group delay equalization, only phase response is of interest, but normally it is impractical to construct an equalizer with inverse phase response of the channel. Instead, a group delay equalizer would be designed to make the total phase response, combined group delay equalizer with the channel to be linear, i.e., $\phi_{total}(\omega) = \phi(\omega) + \phi_{eq}(\omega)$ is proportional to the angular frequency ω. Generally the analog group delay equalizer can be realized by all-pass networks or negative group delay networks.

2.3.1 All-pass networks

An all-pass network (APN) exhibits unit magnitude response over all frequencies, while the associated phase response has a specified feature; thus, all-pass networks are frequently called group delay equalizers.

In order to obtain an all-pass network, the absolute magnitudes of the numerator and denominator of the transfer function must be related by a fixed constant throughout all desired frequencies. It can be achieved by accompanying each pole in the left half plane (for stability) with a mirrored zero in the right half plane as shown in Fig. 2. 7 [26].

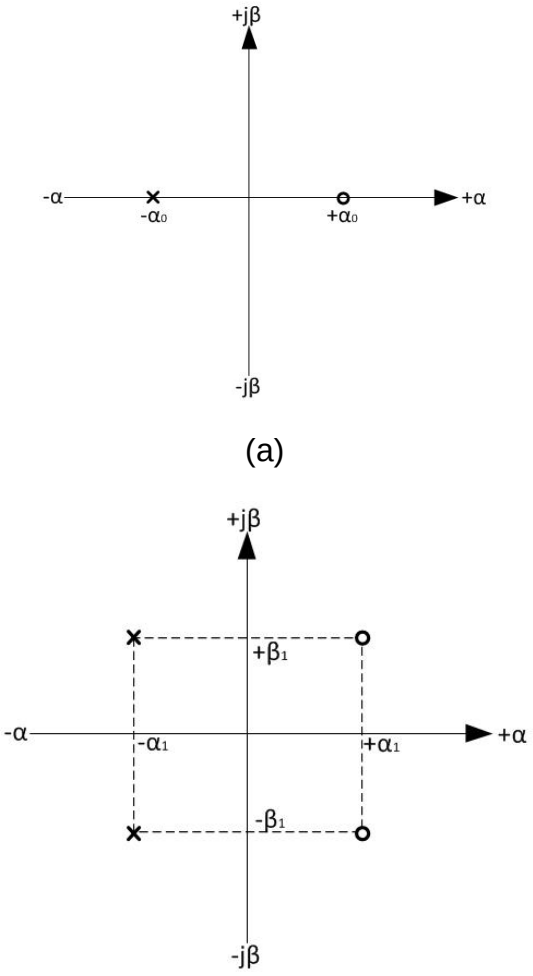

Fig. 2. 7: All-pass pole-zero patterns on S-plane of (a) a first-order all-pass network; and (b) a second-order all-pass network

The transfer function of nth-order AP network can be expressed as

$$H(s) = \frac{S^n + b_1 S^{n-1} + \cdots + a_n}{S^n + a_1 S^{n-1} + \cdots + a_n} \tag{2.18}$$

Since *H*(*s*) is all-pass, the poles and zeros must occur in mirror-image pairs, and a polynomial with real coefficients has roots that must be real or must occur in complex-conjugate pairs. Suppose all poles and zeros of *H*(*s*) are complex except for one real pole and one real zero. After factoring numerator and denominator, *H*(*s*) can be expressed as [5]

$$H(s) = \frac{s - \alpha_1}{s + \alpha_1} \times \frac{(s - \alpha_2)^2 + {\beta_2}^2}{(s + \alpha_2)^2 + {\beta_2}^2} \times \cdots \times \frac{\left(s - \alpha_{(n+1)/2}\right)^2 + {\beta_{(n+1)/2}}^2}{\left(s + \alpha_{(n+1)/2}\right)^2 + {\beta_{(n+1)/2}}^2} \tag{2.19}$$

which is a product of only first- and second-order all-pass functions.

Normally, H(s) can be realized by cascading several first-order or second-order all-pass sections. As a consequence, the total delay is the summation of each section delay. Sections with order higher than two are seldom used, since the number of components is not saved while sensitivity and tuning difficulty are all increased [5].

First-order all-pass networks

The first-order all-pass network, as shown in Fig. 2. 7(a), has one real pole at $-\alpha_0$ and one real zero at $+\alpha_0$. The transfer function can be expressed as

$$H(s) = \frac{s - \alpha_0}{s + \alpha_0} \tag{2.20}$$

where $s = j\omega$.

Checking the absolute value of $H(s)$,

$$|H(s)| = \frac{|j\omega - \alpha_0|}{|j\omega + \alpha_0|} = \frac{\sqrt{\omega^2 + {\alpha_0}^2}}{\sqrt{\omega^2 + {\alpha_0}^2}} = 1 \tag{2.21}$$

For any value of frequency, the numerator of Equation (2.20) is equal to the denominator, resulting in an absolute magnitude of unity at all frequencies.

The phase response is given by

$$\phi(\omega) = -2\tan^{-1}\frac{\omega}{\alpha_0} \tag{2.22}$$

The phase response versus the ratio $\frac{\omega}{\alpha_0}$ is plotted in Fig. 2. 8, where the x-axis is a logarithmic scale. The phase is zero at DC and approaches −180° with increasing frequency.

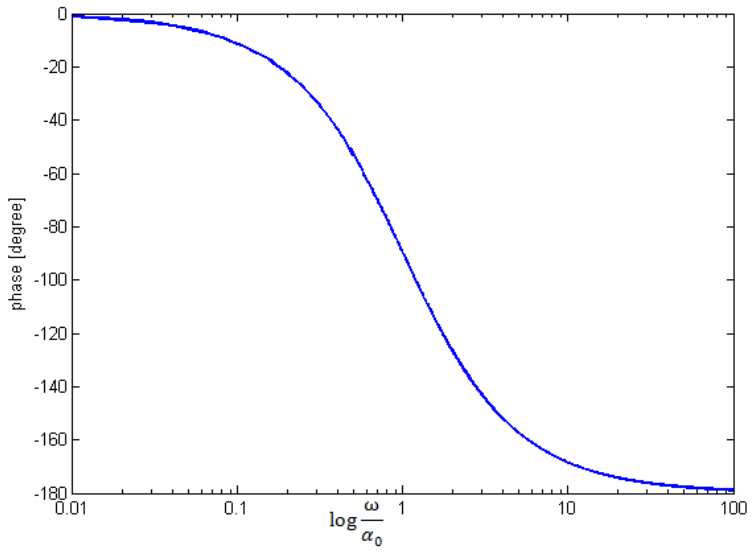

Fig. 2. 8: Phase response of first-order all-pass networks

Then, the group delay can be derived by the definition as

$$\tau_g = -\frac{\partial\phi(\omega)}{\partial\omega} = \frac{2\alpha_0}{{\alpha_0}^2 + \omega^2} \tag{2.23}$$

Plotting the group delay with respect to frequency at different values of α_0 as shown in Fig. 2. 9, it exhibits maximum delay at DC and decreasing delay with increasing frequency. For small values of α_0, the delay becomes large at low frequencies and decreases quite rapidly above this range.

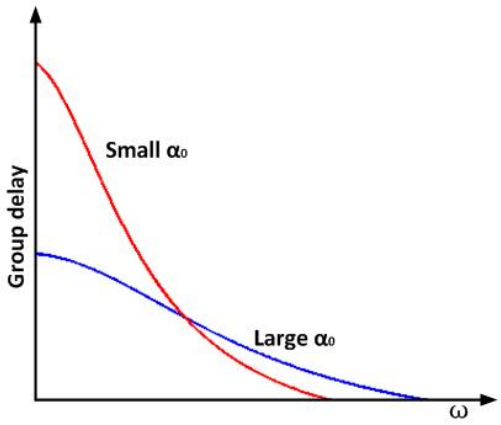

Fig. 2. 9: Group delay of first-order all-pass networks with small α_0 and large α_0

Second-order all-pass networks

The second-order all-pass network, as shown in Fig. 2. 7(b), contains a pair of complex poles $-\alpha_1 \pm j\beta_1$ and mirror-image zeros $\alpha_1 \pm j\beta_1$. The transfer function is

$$H(s) = \frac{(s-\alpha_1)^2 + {\beta_1}^2}{(s+\alpha_1)^2 + {\beta_1}^2} = \frac{s^2 - \frac{\omega_r}{Q}s + {\omega_r}^2}{s^2 + \frac{\omega_r}{Q}s + {\omega_r}^2} \tag{2.24}$$

where ω_r is the pole resonant frequency with value of $\omega_r = \sqrt{{\alpha_1}^2 + {\beta_1}^2}$; Q is the quality factor with value of $Q = \frac{\omega_r}{2\alpha_1}$.

It is also a all-pass network,

$$|H(s)| = \frac{\sqrt{({\omega_r}^2 - \omega^2)^2 + \frac{{\omega_r}^2\omega^2}{Q^2}}}{\sqrt{({\omega_r}^2 - \omega^2)^2 + \frac{{\omega_r}^2\omega^2}{Q^2}}} = 1 \tag{2.25}$$

The phase response is

$$\phi(\omega) = -2\tan^{-1}\left(\frac{\frac{\omega_r\omega}{Q}}{{\omega_r}^2 - \omega^2}\right) \tag{2.26}$$

and the group delay is

$$\tau_g = -\frac{\partial\phi(\omega)}{\partial\omega} = \frac{2Q\omega_r({\omega_r}^2 + \omega^2)}{Q^2({\omega_r}^2 - \omega^2)^2 + {\omega_r}^2\omega^2} \tag{2.27}$$

The typical group delay of second-order all-pass networks is shown in Fig. 2. 10.

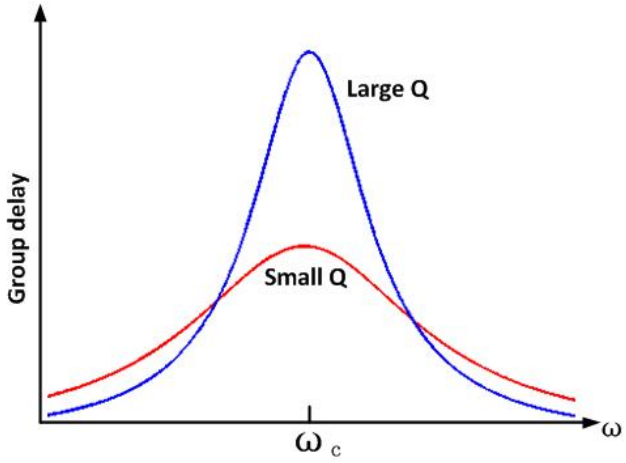

Fig. 2. 10: Group delay of second-order all-pass networks with small Q and large Q

The peak of group delay occurs at the resonant frequency ω_r. As the Q increases, the peak delay also increases and the delay response becomes sharper.

2.3.2 Negative group delay

Instead of increasing over-all group delay, negative group delay (NGD) circuits can be used to suppress the group delay increasing within the desired range. However, recalling the definition of group velocity and group delay, a negative group delay must imply negative velocity. Then, the question might arise as to how a negative group delay or velocity is possible at all. Does it violate the principle of causality?

According to the definition of group delay (Equation (2.13)), negative group delay means that waves of increasing frequency have increasing phase response, i.e., higher frequency wave has less phase change than lower frequency wave [27], as shown in Fig. 2. 11.

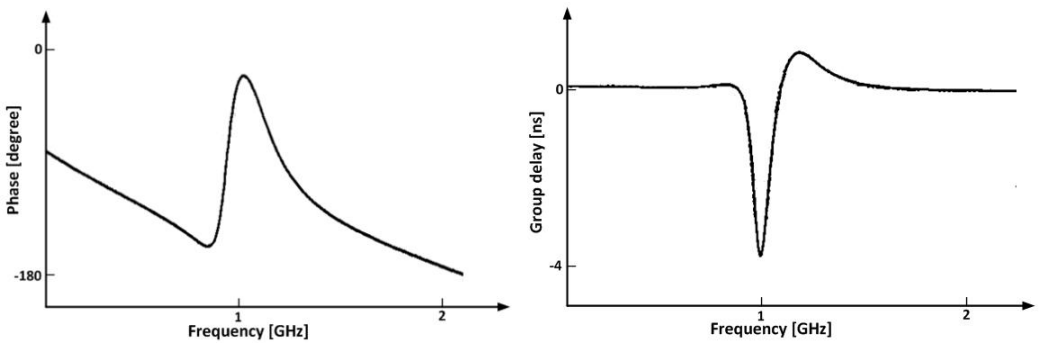

(a) (b)

Fig. 2. 11: (a) Phase response and (b) group delay of a negative group delay circuit

As a consequence of negative group delay, it implies that the peak of output pulse emerges from the media before the peak of input pulse enters as shown in Fig. 2. 12 [28].

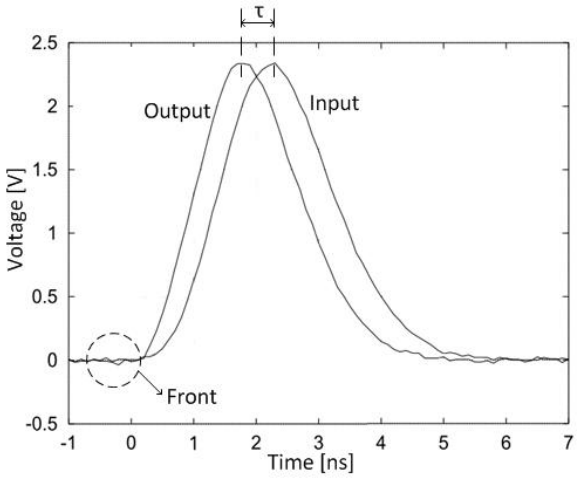

Fig. 2. 12: The traces of output and input pulse transmitted through a NGD circuit

From the above figure, it seems that the output pulse is advanced than the input pulse. However, it does not violate the principle of causality, since the peak in the voltage waveform is not causally related to the one of input pulse. Instead, the causality is solely connected with the occurrence of discontinuities in a signal, e.g., "fronts" and "backs" [29] [30]. Thus, the front of signal must reach the output not earlier than it goes into the input and no signal can precede its front as shown in Fig. 2. 12 where the front of the pulse is marked.

In summary, the negative group delay circuit would only reshape the pulse without violation of the causality. More details about all-pass networks as well as NGD circuits realization would be discussed in chapter 4.

Chapter 3

Effects of group delay variation in filters for communication systems

3.1 Theoretical effects of group delay variation on digital phase modulation

As mentioned in the chapter 2, group delay variation (GDV) will distort the pulse shape for each symbol, resulting the inter-symbol interference (ISI), which would cause serious degradation of the transmission. First, let us analyze the effect of GDV on digital modulations theoretically.

Assuming a pulse shape g(t) with duration in [0, T_s], it is allowed to pass through a system with impulse response $H(\omega) = e^{j\phi(\omega)}$ which has the constant amplitude. Then the output pulse $\hat{g}(t)$ can be expressed as

$$\begin{aligned} \hat{g}(t) = g(t) * h(t) &= \int_{-\infty}^{+\infty} G(\omega)\, H(\omega) \cdot e^{j\omega t} d\omega \\ &= \int_{-\infty}^{+\infty} G(\omega)\, e^{j\omega t} e^{j\phi(\omega)} d\omega \end{aligned} \tag{3.1}$$

where $G(\omega)$ and $H(\omega)$ are the Fourier transforms of $g(t)$ and $h(t)$ respectively. When $\phi(\omega)$ is linear respect of the angular frequency ω, i.e., $\phi(\omega) = -a_0\omega$, where a_0 is a constant, it is easy to obtain that the output pulse $\hat{g}(t)$ is delayed waveform of $g(t)$, i.e., $\hat{g}(t) = g(t - a_0)$. As shown in Fig. 3. 1(a), the output pulse is exactly the same as the input pulse except the delay.

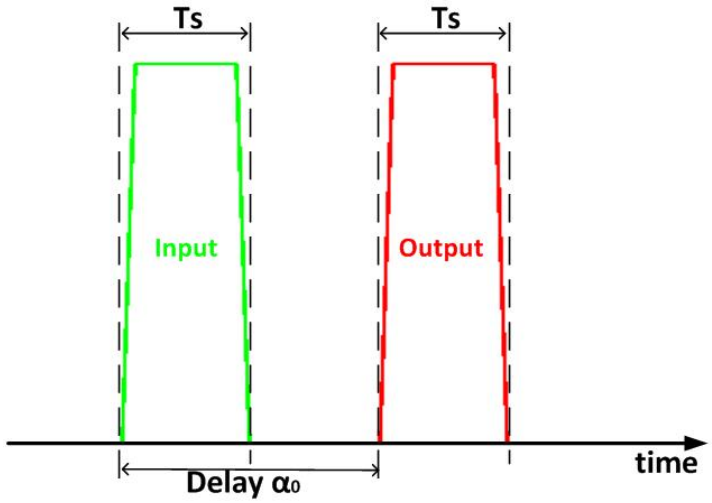

(a)

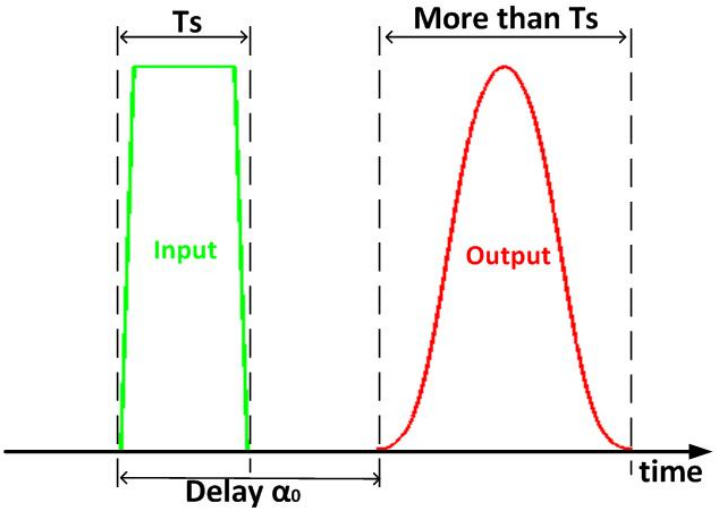

(b)

Fig. 3. 1: Input and output pulse in time domain going through channels with (a) linear phase response and (b) non-linear phase response

However, if the phase response in non-linear, it contains higher order terms (i.e., $\omega^2, \omega^3 \cdots$). As a consequence, the output pulse is not only delayed but also distorted and normally it would be broadened comparing with the original one as show in Fig. 3. 1(b). It can be seen that the duration of the output pulse for one symbol exceeds the symbol interval T_s, which would make neighboring pulse overlapped resulting in the inter-symbol interference.

In general, it can be concluded that ISI is one of the effect of GDV on digital communications, which can be easily observed through eye diagrams as well as the constellation.

3.1.1 Eye diagram

Eye diagram is a useful graphical illustration to evaluate the degradation of the signal, so called because its shape is similar to one of human eyes [31]. An eye diagram can be generated by an oscilloscope to observe the output signal and overlap traces of a signal within a certain period (normally it is chosen to be 2Ts, i.e., two symbol intervals) as shown in Fig. 3. 2. If the data symbols are independent and long enough, it can present all possible degradation of signal due to the impairment of channels.

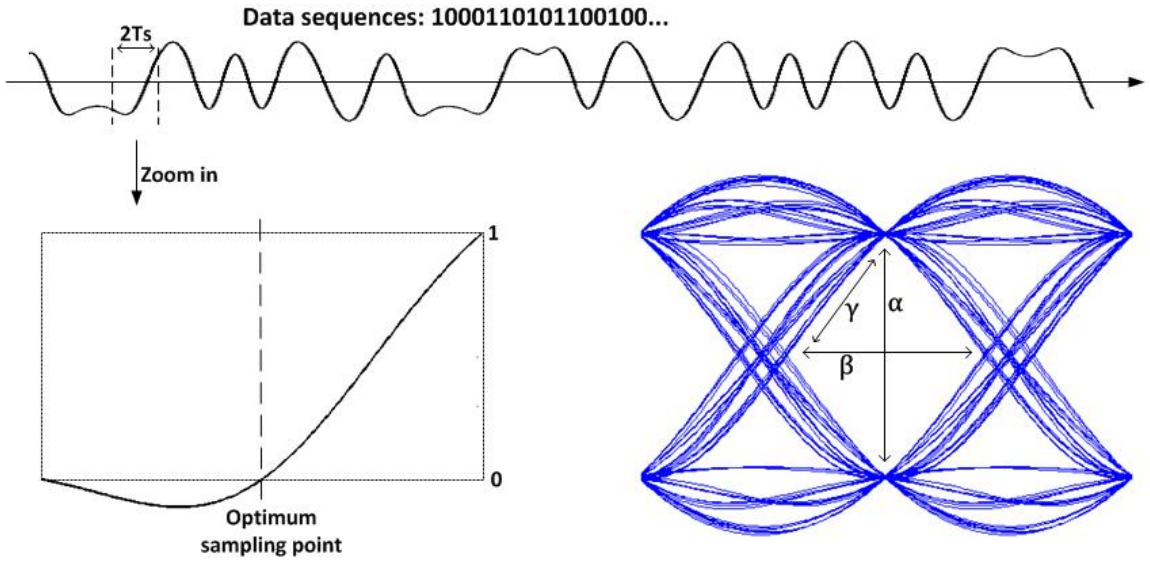

(a) (b)

Fig. 3. 2: (a) Data sequence wave form and one detailed circle of length 2Ts with raised-cosine pulses; (b) typical eye diagram with salient features

As shown in Fig. 3. 2(b), α indicates the vertical eye opening, which also represents the immunity to the noise. The optimum sampling point is at the instant when the vertical eye opening is maximum. However, it is can never be achieved due to the imperfection of timing recovery circuit. Thus, the horizontal eye opening is also important representing the immunity to errors in the timing phase which is

marked by β. The slope γ between them indicates the sensitivity to jitter in the timing phase [31].

According to the Nyquist criterion, if data is shaped by Nyquist pulse, there is no inter-symbol interference in the transmission. However, if the systme contains group delay variation, the pulse would be reshaped and the Nyquist criterion is no longer satisfied, resulting in the ISI, which can reduce both the vertical and horizontal eye opening. In cases of severe ISI, the eye would even close completely as shown in Fig. 3. 3.

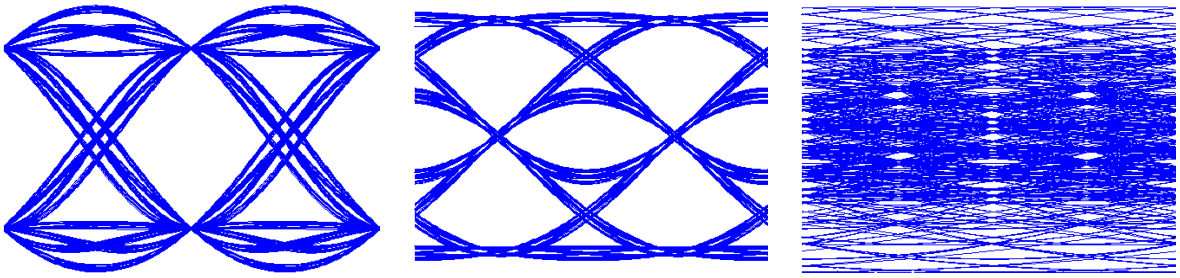

(a) (b) (c)

Fig. 3. 3: Eye diagrams (a) without GDV, (b) with small GDV ($2.5T_s$) and (c) with large GDV ($8T_s$) in absence of noise where GD is modeled as linear

3.1.2 Constellation

Constellation diagrams are used to visualize the received signal with modulation formats, which provide information about both the amplitude and the phase. In QPSK, also known as 4QAM, the base band signal can be written as

$$s_k(t) = g(t)e^{j\theta_k}, \theta_k = \frac{\pi}{2}\left(i - \frac{1}{2}\right), i = 1,2,3,4 \tag{3.2}$$

Thus, each symbol can be expressed as a vector:

$$s_k = [s_{k1}, s_{k2}] = [\sqrt{E_s}\cos\theta_k, \sqrt{E_s}\sin\theta_k] \tag{3.3}$$

where E_s is the average energy of the symbol and θ_k indicates one of 4 possible phases [24]. Plotting all possible symbols on the complex plane, the constellation is produced as Fig. 3. 4.

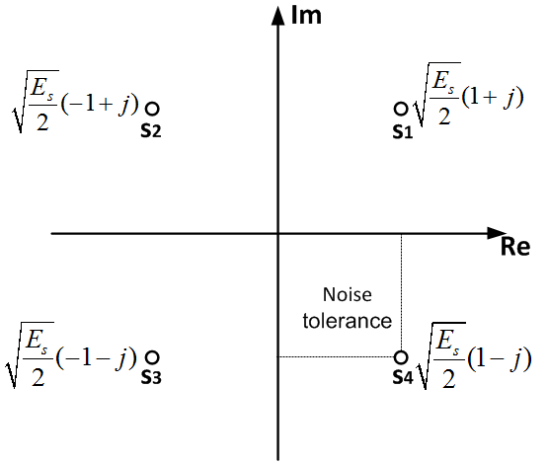

Fig. 3. 4: Constellation plot for QPSK (4-QAM)

As shown in Fig. 3. 4, the real and imaginary axis divide the complex plane into 4 areas, each of which represents a certain symbol. Hence, if one received symbol locates in a certain area, it would be judged to be the corresponding symbol. Due to the existence of noise, the received symbol has chance to locate in other areas, which would cause the error after the decision.

When transmitting the signal through a channel with group delay variation, the received symbol can be modified by a displacement in the constellation [32]. Hence, the received symbol can be expressed as

$$r_k = [s_{k1} + a,\ s_{k2} + b] \tag{3.4}$$

where a and b is characterized parameter depending on both the type and the value of GDV.

As shown in Fig. 3. 5, the received symbol is shifted from the original one due to the group delay variation. As a consequence, the received symbol is closer to other possible symbols and the noise tolerance is reduced, which would degrade the performance of the transmission especially for the high modulation format, e.g., 64QAM and 256QAM.

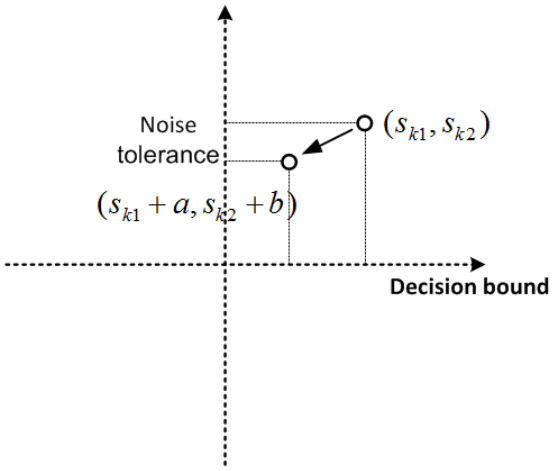

Fig. 3. 5: Displacement of received symbol and transmitted symbol

3.2 Simulation platform

An exact analysis of GDV effects in practical systems is rather difficult while it is simpler to simulate it in *MATLAB*. Since the effect of the linear group delay (also called chromatic dispersion) in optical fibers has been widely investigated and discussed in optical communications, this work will mainly focus on the effect of GDV in different types of band-pass filters, such as Chebyshev, Elliptic, Butterworth, etc..

3.2.1 Block diagram

The block diagram of simulation platform is shown in Fig. 3. 6.

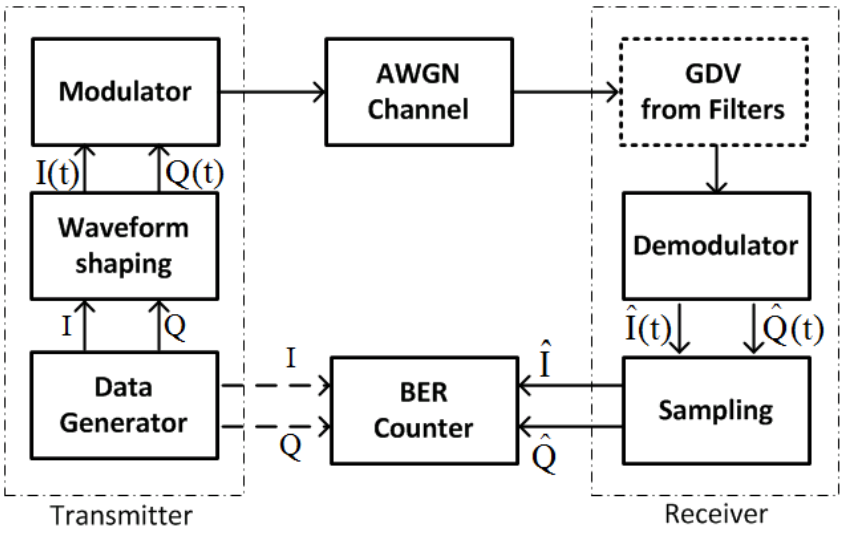

Fig. 3. 6: The block diagram of simulation platform

As the discussion in section 3.1, the eye-diagram as well as the constellation can be used to evaluate the effect of GDV. However, in order to compare the degradation of different GDVs quantitatively, the figure of bit error rate (BER) versus signal to noise ratio (SNR) would be used.

A random bit sequence (I and Q) is sent from the transmitter through the channel and compared with the detected sequence ($\hat{I}$ and $\hat{Q}$) in the receiver (BER counter). The incorrectly identified bits are regarded as bit errors, then the BER can be defined as

$$BER = \frac{number\ of\ bit\ errors}{number\ of\ transmitted\ bits} \tag{3.5}$$

Due to the stochastic nature of channel, the BER is usually related to the bit error probability. When measuring the BER for a sufficiently long sequence, the value of BER would approach to the bit error probability, which represents the expected value for a certain signal to noise (SNR). Thus, in order to obtain the bit error probability with acceptable accuracy, normally at least 100 errors are required to evaluate the BER, e.g., for measuring BER with expectation of 10^{-5}, $\frac{100}{10^{-5}} = 10^7$ bits should be transmitted and compared.

Additive white Gaussian noise (AWGN) channel model is used in the simulation, which means the only impairment is a linear addition of white noise with a constant spectral density and a Gaussian distribution of amplitude [33], i.e., $n \sim N\left(0, \frac{N_0}{2}\right)$ for

real and imaginary domain respectively, so that the total power spectral density of noise is N_0 . Then the signal to noise (SNR) ratio can be defined as [31]

$$SNR = \frac{E_s}{N_0} \tag{3.6}$$

where E_s is the average energy of one symbol.

Hence, by changing the symbol energy with fixed power density of noise, the SNR can also be changed correspondingly, and consequently different BERs (normally higher SNR results in lower BER) are obtained.

All data is shaped by root-raised-cosine pulse with the roll-off factor of 0.25 accompanying by a matched filter (also is root-raised-cosine pulse) in the receiver, so that the output waveform satisfies the Nyquist criterion in the absence of GDV [24]. Also, it can make the transmitter signal band-limited within certain range, which would eliminate the effect of the selectivity of filters.

The GDV in filters is added in the front of the receiver. As the discussion in Section 3.1, the GDV would increase the bit error rate. It can also be understood by setting a target of BER, and measuring how much SNR is needed to achieve that target. Thus, the GDV would increase the requirement of SNR (increasing transmit power if the noise is stable). Comparing with the case without GDV, the extra power can be defined as the penalty power caused by GDVs in order to achieve the same performance in terms of BER.

3.2.2 Group delay of filters under test

As mentioned in chapter 2, GDV in pass-band filters would only occur at the edge of the pass band. In the simulation, the carrier frequency is set to be 10 GHz with the bandwidth of 5 GHz. Thus, in order to evaluate the effect of GDV, the transmitted signal needs to occupy the whole passband (7.5 - 12.5 GHz).

The amplitude response and GDV of filters with different types are present in Fig. 3. 7.

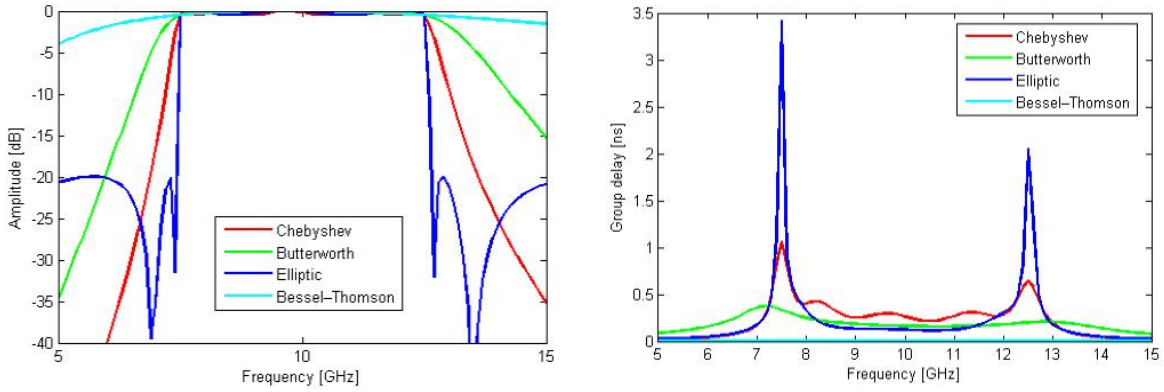

(a) (b)

Fig. 3. 7: (a) Amplitude response and (b) group delay response of filters with same order of 5 but different type (simulation results from the ideal filter components in ADS, stopband rejection for Elliptic is 20dB)

It can be seen that the elliptic filter has best selectivity when the filter order is kept as the same, while its GDV is also maximum at around 3.4 ns. The Chebyshev filter has the second largest GDV with the peak of 1 ns and good selectivity while the Butterworth filter has both moderate GDV and selectivity. In addition, the Bessel-Thomson filter, also called maximally flat group delay filter, has the worst performance on the selectivity, but its GDV can be ignored comparing with ones of other filters.

Above all, it can be concluded that normally a steep filter edge would cause a large group delay variation. It would be a trade-off between the GDV and the selectivity when designing filters for communication systems.

The effect of GDV with different filters will be evaluated based on 4QAM and 16QAM modulation respectively.

3.3 Simulation results

The BER versus SNR with different filters for 4QAM is shown as Fig. 3. 8.

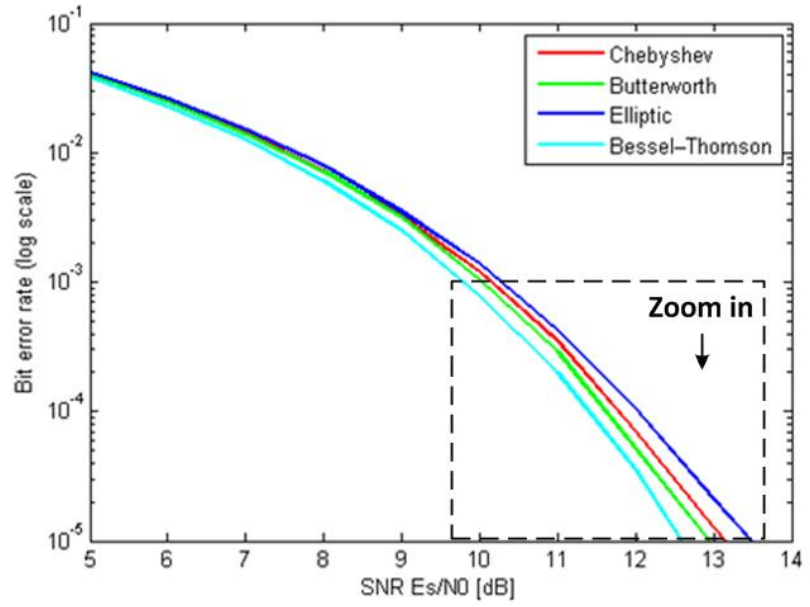

(a)

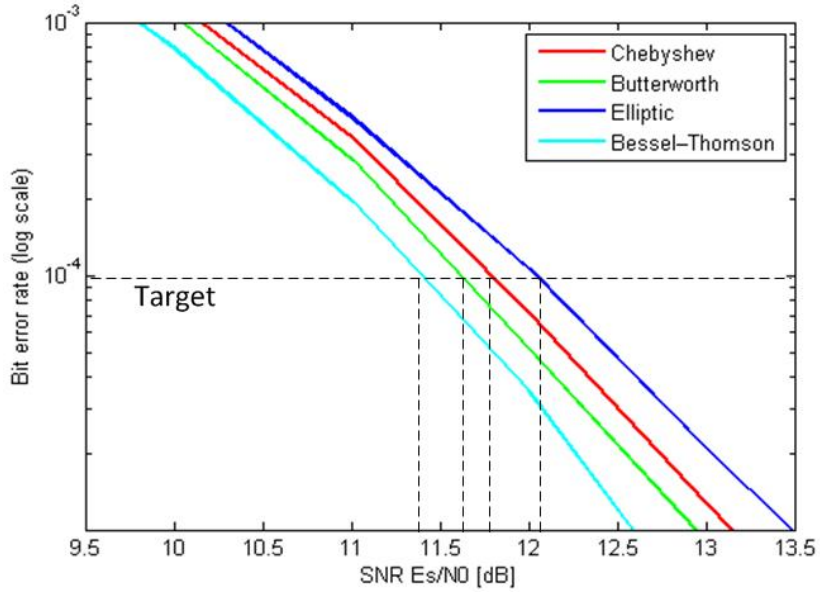

(b)

Fig. 3. 8: (a) Bit error rate versus SNR with different filters for 4QAM and (b) the zoom-in plot

It can be seen that the Bessel-Thomson filter has the best performance in terms of the bit error rate. That is reasonable since it has almost a flat group delay which means a linear phase response. As the discussion in section 3.1, the output pulse would be kept as exactly same as the original one, so that its performance is similar to the case with AWGN channel only, which could be a reference to evaluate other types of filters.

It also shows that larger GDV has a worse performance. Setting a target of BER to 10^{-4} as shown in Fig. 3. 8(b), it can be see that for Bessel-Thomson filter 11.3 dB SNR is required to achieve the target while for Elliptic filter 12.1dB is needed which means extra 0.7 dB power has to be paid for the GDV. The penalty power for Chebyshev and Butterworth filter is 0.3 dB and 0.5 dB respectively. It can be found that the GDV of filters has little effect on the performance with maximum penalty power of 0.7 dB. The reason for is that for 4QAM modulation, the spectral efficiency is still low and the effect of GDV can be ignored compared to that of Gaussian noise.

Similarly, The BER versus SNR with different filters for 16QAM is plotted in Fig. 3. 9.

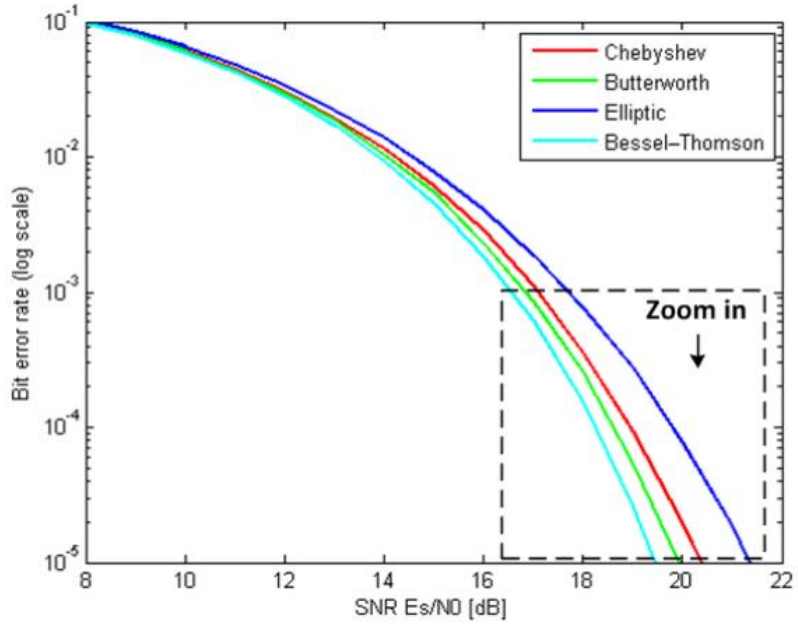

(a)

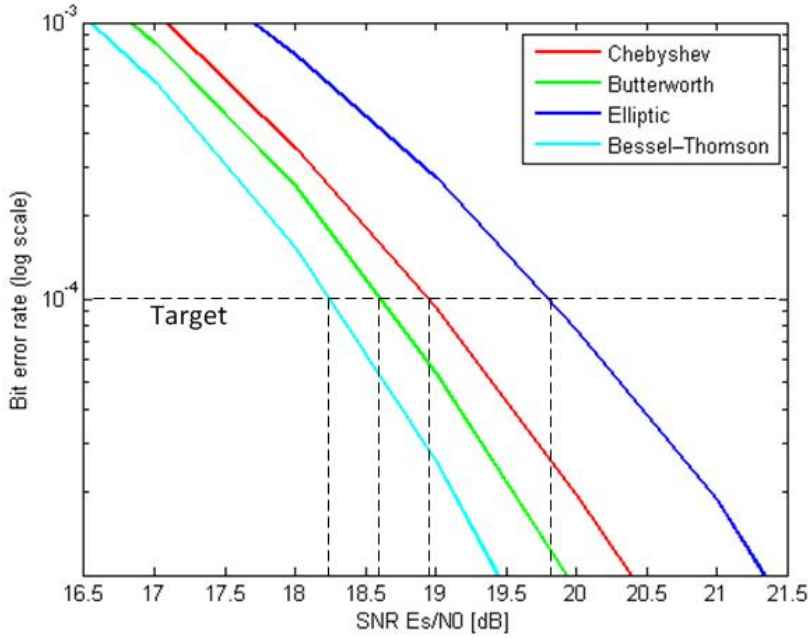

(b)

Fig. 3. 9: (a) Bit error rate versus SNR with different filters for 16QAM and (b) the zoom-in plot

It can be seen that the effect of GDV on 16QAM is similar to the one on 4QAM. However, the penalty power is increased. In order to achieve the BER of 10^{-4}, 18.2 dB SNR is needed for Bessel-Thomson filter while Elliptic filter requires 19.8 dB. More details about the performance of filters are summarized in Table 3.1.

Type of filter		AWGN	Bessel-Thomson	Butterworth	Chebyshev	Elliptic
Peak of GDV (ns)		/	Almost 0	0.4	1.1	3.4
4QAM	SNR for BER of 10^{-4} (dB)	11.3	11.3	11.6	11.8	12.1
	Penalty power (dB)	/	Almost 0	0.3	0.5	0.8
16QAM	SNR for BER of 10^{-4} (dB)	18.2	18.2	18.6	18.9	19.8
	Penalty power (dB)	/	Almost 0	0.4	0.7	1.6

Table 3.1: Summary of performance of filters for 4QAM and 16QAM

It can be concluded that the GDV in band-pass filters has less effect on the performance of communication system with low-order modulation, since the bandwidth efficiency is low and only a little signal locates in the transition area. In 4QAM case, the Elliptic filter with maximum group delay variation, which has the best selectivity, can only cause the penalty power 0.7 dB. Thus, group delay equalization is of no need.

On the other hand, for systems using high-order modulation with high power spectral efficiency, such as 16QAM, the GDV would cause the penalty power with several dB, so that the effect of GDV needs to be taken into consideration. In addition, for some special cases, such as satellite communication and audio signal processing, the requirement for preservation of the waveform is highly restricted. As a consequence, the group delay equalization is necessary.

Chapter 4

Group delay equalization methodologies for filters

In this chapter, several methodologies of group delay equalization based on electronic circuits will be discussed and compared. Generally, group delay equalization for filters can be implemented by two methods: second-order all-pass networks and negative group delay circuits. As shown in Fig. 4. 1, the second-order all-pass network generates a positive group delay variation with a convex feature (Fig. 4. 1(b)), which is opposite to the one of band-pass filters. Consequently, the overall circuit contains an almost flat group delay response in the desired frequency range while the total group delay time is increased.

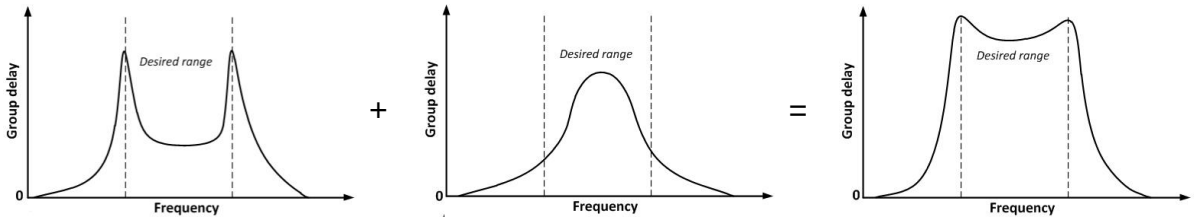

(a) (b) (c)

Fig. 4. 1: Group delay response of (a) a band-pass filter, (b) a second-order all-pass network and (c) the overall circuit

Instead of increasing total group delay time, negative group delay circuits can be used for group delay equalization as shown in Fig. 4. 2. It can be seen that two peaks of group delay variation in the band-pass filter are reduced owing to the negative group delay circuit, while the total group delay time is just slightly increased.

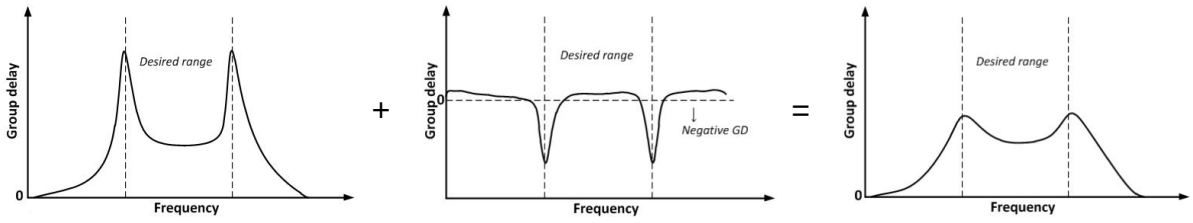

(a) (b) (c)

Fig. 4. 2: Group delay response of (a) a band-pass filter, (b) a negative group delay circuit and (c) the overall circuit

Section 4.1 and 4.2 show all-pass networks implemented by lumped elements and distributed elements respectively. Section 4.3 shows negative group delay circuits; while a novel equalization method is proposed in Section 4.4, which is based on reflection-type negative group delay circuits with negative resistance.

4.1 All-pass networks with lumped elements

In chapter 2, two types of all-pass networks (APNs) are described, namely, those of first and second order. However, only the second-order type of APN could be a suitable building block for group delay equalization [34]. In analog circuits, the basic section of the second-order APN can be implemented by lumped-elements, i.e., inductors and capacitors, as shown in Fig. 4. 3 [5] [26].

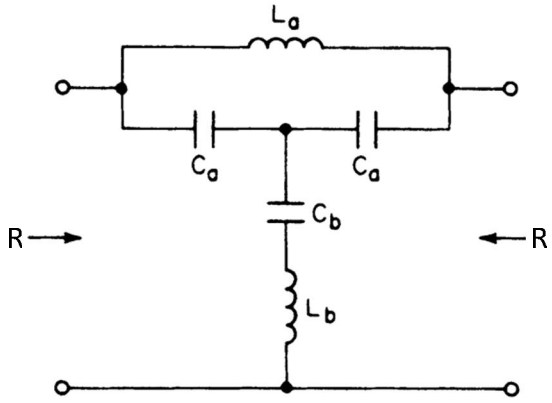

Fig. 4. 3: Second-order all-pass section

The design equations are given in [26] and [5] as follows:

$$\omega L_a = 2kR \tag{4.1}$$

$$\omega C_a = \frac{1}{kR} \tag{4.2}$$

$$\omega L_b = \frac{R}{2k} \tag{4.3}$$

$$\omega C_b = \frac{2k}{[\frac{R}{(1-k^2)}]} \tag{4.4}$$

where *R* is the value of terminating impedance (normally 50 Ohm) and *k* is a factor in the range of 0 to 1 that determines the peak group delay τ at the resonant frequency ω according to

$$\tau = \frac{4}{k\omega} \tag{4.5}$$

Theoretically, the second-order all-pass section has an all-pass property, which means its amplitude response is a unit over all frequencies. Unfortunately, real lumped components have not only imaginary reactive impedances the but also a small amount of real resistive ones, which would cause the loss, especially at the resonant frequency.

The performance of several all-pass sections consisting of lumped elements with different inductor quality factors (Q) are shown in Fig. 4. 4. It is clear to see that lower Q value would cause larger attenuation. A typical quality factor for inductors implemented in the monolithic microwave integrated circuit (MMIC) is smaller than 30 at frequency larger than 10 GHz, which would cause more than 6 dB loss at the resonant frequency 15 GHz. The all-pass section with Q=300 can achieve the loss around 0.6 dB. However, the quality factor has less effect on the peak of group delay, which is 0.42ns and 0.48ns in cases Q=300 and Q=30, respectively.

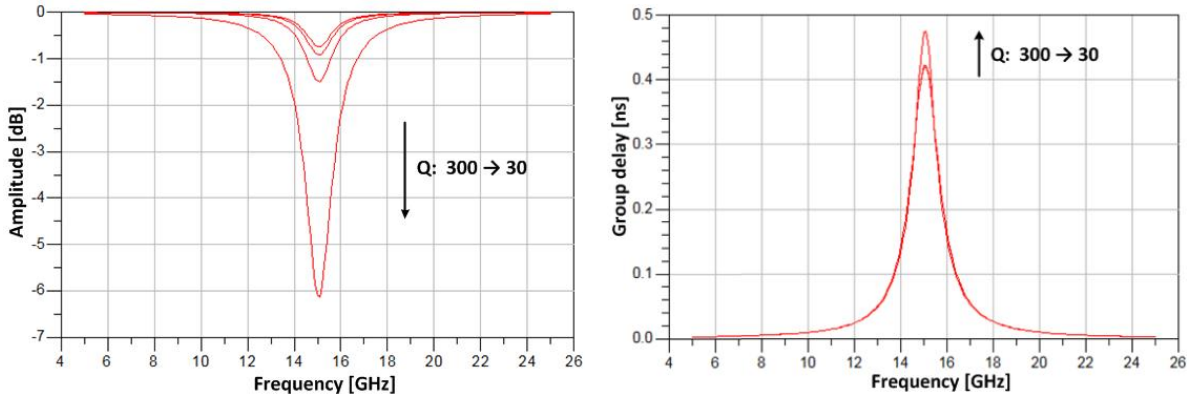

(a) (b)

Fig. 4. 4: The amplitude response (a) and group delay response (b) of the second-order all-pass section with different quality factor (Q: 30-300)

In addition, the conventional APN has another problem which is related to the manufacture and selection for lumped components. According to the equations (4.1)-(4.4), the ratio of inductors and capacitors can be obtained as [34]

$$\frac{L_b}{L_a} = \frac{1}{4k^2} \tag{4.6}$$

$$\frac{C_a}{C_b} = \frac{1-k^2}{2k^2} \tag{4.7}$$

From the equation (4.5), it can be seen that lower *k* would cause higher peak delay. In majority cases, *k* is chosen to be less 0.1, which means the inductor ratio is larger than 25 while the capacitor ratio is more than 50. Such large ratios would cause the difficulty to select or manufacture such passive components. In [34], an improved topology for second-order APNs is proposed, overcoming these disadvantages. However, the loss is still a remaining issue.

As the conclusion, the performance of the all-pass network is limited by the quality factor of lumped components, Normally the quality factor more than 300 is required, which can be satisfied by discrete lumped components mounted on printed circuit board (PCB). For MMIC implementation, the compensation for the loss of the all-pass network has to be taken into consideration [35].

4.2 All-pass networks with distributed implementation

Unlike the lumped elements, distributed elements are more flexible to design the all-pass network, but they consumes much more chip/motherboard area. The all-pass network based on distributed elements was first proposed in 1970s [36] and demonstrated for narrowband phase-shifting applications. In 2010, group delay networks are proposed based on noncommensurate (different lengths of lines) transmission lines [3]. The basic section, which is also called C-section, is the shorted coupled-line pair as shown in Fig. 4. 5.

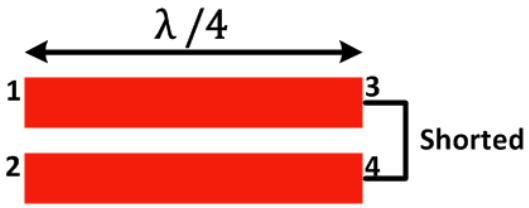

Fig. 4. 5: Coupled transmission line all-pass networks with port 3 and 4 shorted

The length of two transmissions are the same and they are equal to a quarter wavelength at the center frequency. Port 3 and port 4 are shorted/connected. Thus, it can be regarded as a two-port network. Its transfer function can be expressed as [3]

$$S_{21}(\theta) = \frac{\sqrt{1+k}cos\beta l - j\sqrt{1-k}sin\beta l}{\sqrt{1+k}cos\beta l + j\sqrt{1-k}sin\beta l} \tag{4.8}$$

where β is the propagation constant of the transmission line and l is the length. k is the coupling coefficient with value between 0 and 1.

It would be easy to verify that it is an all-pass section due to $|S_{21}(\theta)| = 1$. Also the group delay can be obtained by the equation (2.13) as

$$\tau_g = -\frac{\partial \angle S_{21}}{\partial \omega} = \frac{2a}{a^2 + (1-a^2)cos^2\theta}\frac{d\theta}{d\omega} \tag{4.9}$$

where $a = \sqrt{\frac{1-k}{1+k}}$ and the θ is the electrical length with value of βl [3].

A typical group delay response is as shown in Fig. 4. 6.

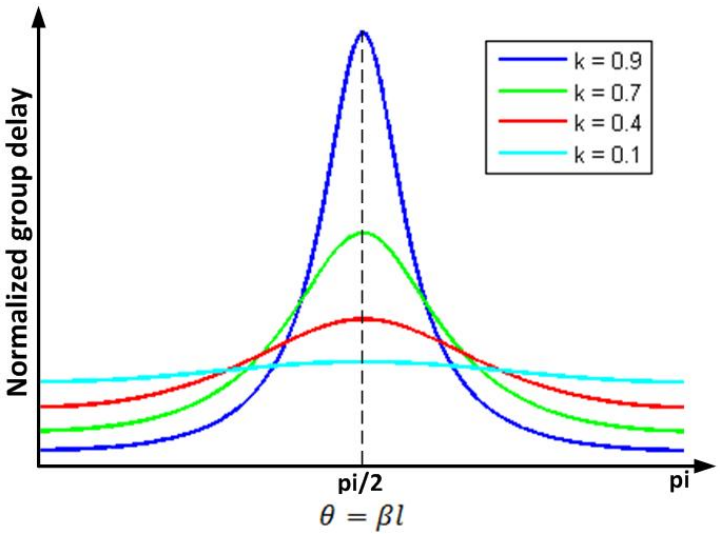

Fig. 4. 6: Group delay of distributed APNs versus the electrical length and the coupling factor k.

It can be found that the characteristic of group delay variation is same as that of the second-order all-pass network with a peak at the resonant frequency ($\theta = \frac{\pi}{2}$). As k increases, which means stronger coupling, the peak of group delay would also increase while the bandwidth decreases. By cascading several stages of such all-pass sections with different resonant frequencies, the bandwidth can be increased and even quasi-arbitrary group delay response might be synthesized [3].

However, for edge-coupled transmission lines the coupling strength is limited by the PCB layout, since the minimum distance between two lines is restricted. Thus, an APN based on edge-coupled lines usually suffers from a large size and limited group delay variation. Consequently, an all-pass network based on broadside-coupled striplines is proposed [37] , in order to enhance the coupling as well as increase the group delay swing. However, due to the loss in the transmission line, a large attenuation would occur at the resonant frequency as shown in Fig. 4. 7, which is similar to the case in all-pass networks with lumped elements.

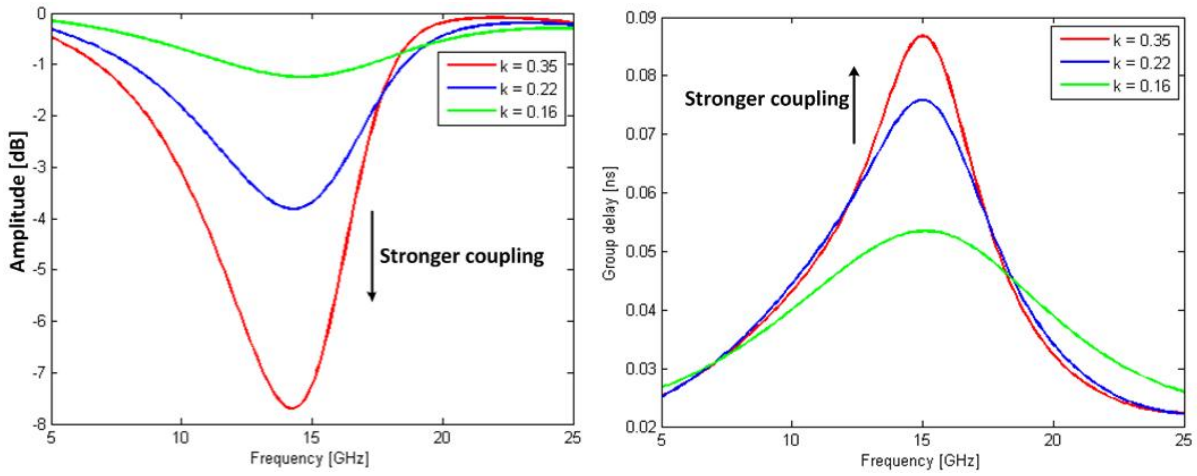

(a) (b)

Fig. 4. 7: The amplitude response (a) and group delay response (b) of the APN consisting of coupled microstrip lines on substrate with ϵ_r = 2.3, TanD=0.001; varied by the coupling factor *k* (0.16, 0.22, 0.35)

Comparing with Fig. 4. 5, it is clear to find that the distributed all-pass network has a larger bandwidth than that of lumped all-pass network while the peak of the group delay is much smaller at around 0.085 ns for the case with coupling factor 0.35. Normally all-pass networks with stronger coupling would cause larger attenuation. Thus, in realistic implementation of distributed APNs, the coupling factor is limited to be a low number while the value of group delay variation is also limited. Furthermore, a substrate with low loss can be chosen to implement transmission lines to decrease the loss and improve the performance of APNs.

4.3 Negative group delay circuits

As the discussion in section 2.3.3, negative group delay (NGD) circuit would not violate the principle of causality; instead, it only reshapes the waveform of the pulse. Two typical topologies for NGD circuits are shown in Fig. 4. 8.

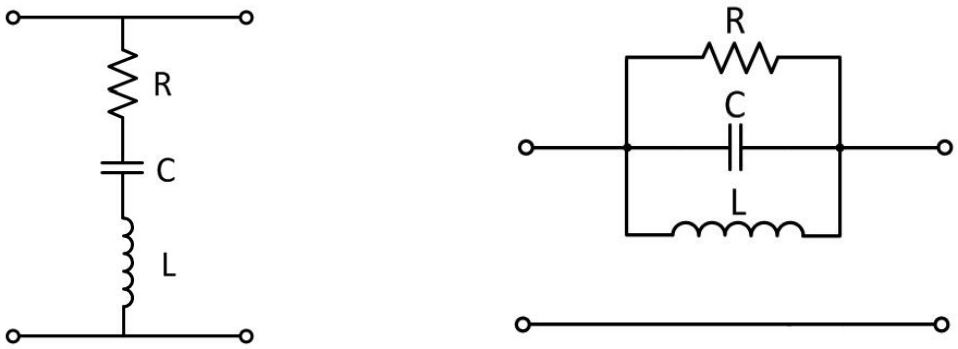

(a) (b)

Fig. 4. 8: Typical NGD circuits with (a) shunt-series resonance (SSR); and (b) series-parallel resonance (SPR) [18]

In Fig. 4. 8, both NGD circuits are two-port network: one is using shunt-series resonance (SSR) and the other is using series-parallel resonance (SPR) [38] [18]. By terminating both ports with load Z_0, the transmission coefficient (S_{21}) for both circuits can be calculated as [39]:

$$S_{21,SSR} = \frac{2R + 2(j\omega L + \frac{1}{j\omega C})}{Z_0 + 2R + 2(j\omega L + \frac{1}{j\omega C})} \tag{4.10}$$

$$S_{21,SPR} = \frac{2Z_0(\frac{1}{R} + \frac{1}{j\omega L} + j\omega C)}{2Z_0\left(\frac{1}{R} + \frac{1}{j\omega L} + j\omega C\right) + 1} \tag{4.11}$$

where ωL is equal to $\frac{1}{\omega C}$ at the resonance frequency and Z_0 is the load impedance with normal value of 50 Ohm.

The minimum valley of the group delay also occurs at the resonance frequency. Thus, based on the group delay definition and the equation $\omega L = \frac{1}{\omega C}$, the minimum group delay for SSR circuits can be obtained:

$$\tau_{g,SSR}\big|_{\omega=\omega_0} = -\frac{\partial \angle S_{21,SSR}}{\partial \omega}\bigg|_{\omega=\omega_0} = -\frac{2Z_0 L}{R(2R + Z_0)} \tag{4.12}$$

and for SPR circuits:

$$\tau_{g,SPR}\Big|_{\omega=\omega_0} = -\frac{\partial \angle S_{21,SPR}}{\partial \omega}\Big|_{\omega=\omega_0} = -\frac{2R^2C}{2Z_0 + R} \tag{4.13}$$

It is simple to prove that the group delay for both circuits are negative when R, C and L are positive. Fig. 4. 9 shows the typical amplitude response and group delay for the SPR circuit plotted in Fig. 4. 8(b), where inductance and capacitance are 0.23 nH and 0.49 pF, respectively, and the resistance is 150, 250 and 350 Ohm.

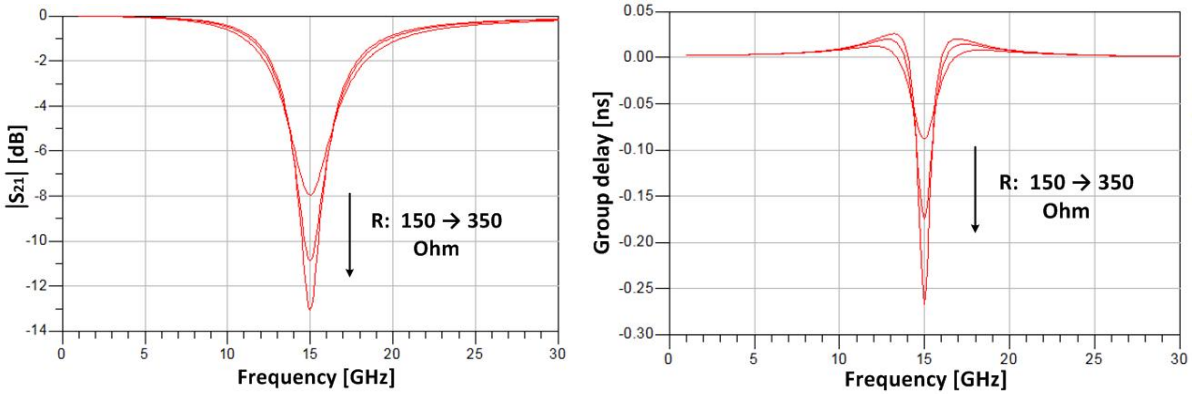

(a) (b)

Fig. 4. 9: (a) The amplitude response of S_{21} and (b) group delay for the SPR circuit shown in Fig. 4. 8(b) (L=0.23 nH, C=0.49 pF, R=150, 250, 350 Ohm)

It can be seen that within the frequency from 13.5 GHz to 15.5 GHz the circuits have negative group delay with minimum value at 15 GHz. However, it also can be seen that the gain drop at 15 GHz is a companion to negative group delay. Normally, a larger resistance (e.g., 350 Ohm) would cause a larger group delay variation (with minimum NGD around -0.26 ns) while it also cause a larger attenuation (13 dB). Thus, in order to make use of NGD circuits, the amplitude compensation is necessary.

In [40], an active negative group delay (ANGD) circuit is proposed, where the amplifier is used to increase the gain, as shown in Fig. 4. 10. However, this amplifier increases gain over a broad frequency range, as shown in Fig. 4. 11(a); in other words, the gain increase caused by using amplifier is not limited to the frequency range where the negative group delay occurs. In this example, the negative group delay occurs at frequency around 1 GHz, but the amplitude of S_{21} has also a minimum point at this frequency with value of 4 dB. The variation of the amplitude of S_{21} is an undesired feature [41]. In next section, a novel negative group delay circuit with reflection amplifier will be proposed, in order to achieve a flat gain within a wide frequency range.

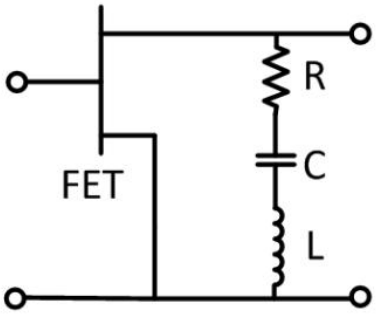

Fig. 4. 10: Active negative group delay (ANGD) circuits

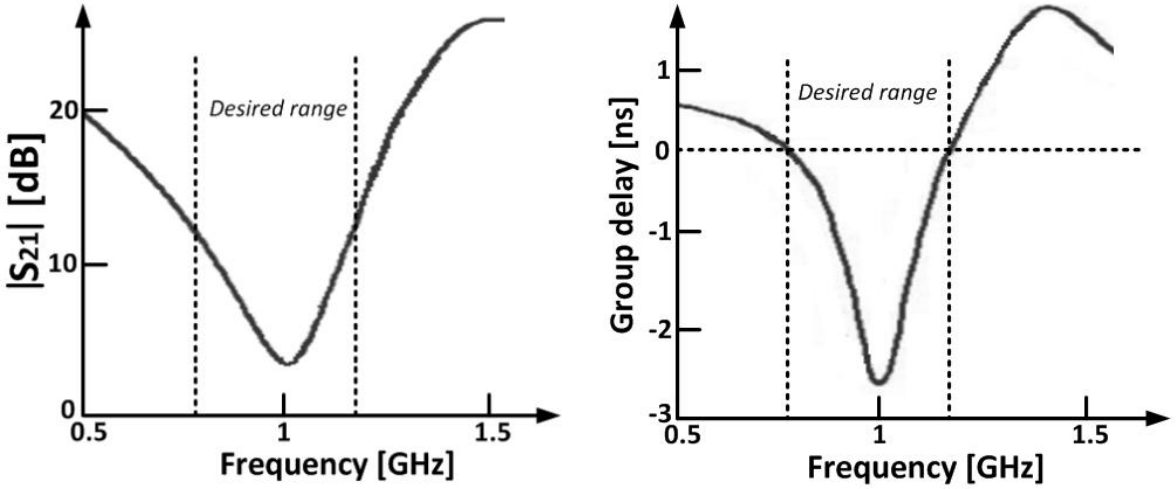

(a) (b)

Fig. 4. 11: (a) The amplitude response of S_{21} and (b) group delay response of active negative group delay (ANGD) circuits [40]

4.4 NGD circuits with negative resistance

NGD circuits discussed in section 4.3 can be called transmission-type NGD circuits, since the transmission signal (S_{21}) is used. Normally they would have some problems in broadband matching, resulting in the narrow bandwidth. Instead, the reflection-type NGD (RNGD) circuits, which means the reflected signal S_{11} would be used, can be designed to overcome the bandwidth limitation [42].

4.4.1 Reflection-type NGD circuits

The topology for reflection-type NGD circuits is plotted in Fig. 4. 12.

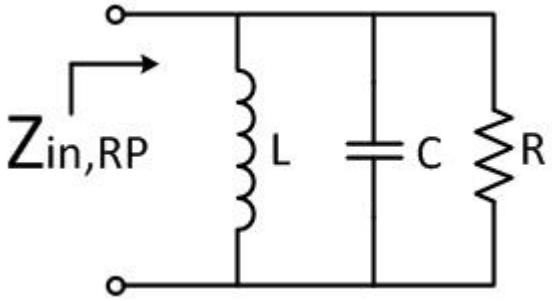

Fig. 4. 12: The reflection-type negative group delay circuit with a parallel resonator

Basically it is a parallel RLC resonator and its input admittance can be represented as

$$Y_{in,RP} = \frac{1}{Z_{in,RP}} = \frac{1}{R} + j\omega C + \frac{1}{j\omega L} \tag{4.14}$$

Then, the reflection coefficient Γ_{RP} can be derived as follows [42]:

$$S_{11,RP} = \Gamma_{RP} = \frac{Y_0 - Y_{in,RP}}{Y_0 + Y_{in,RP}}$$

$$= \frac{Y_0 - \frac{1}{R} + j(\frac{1}{\omega L} - \omega C)}{Y_0 + \frac{1}{R} + j(\omega C - \frac{1}{\omega L})} \tag{4.15}$$

where Y_0 is the load admittance, usually, its value is 20 mS corresponding to 50Ω.

The phase response of S_{11} can be expressed as

$$\angle S_{11,RP} = \tan^{-1}\left[\frac{(1-\omega^2 LC)R}{(Y_0 R - 1)\omega L}\right] - \tan^{-1}\left[\frac{(\omega^2 LC - 1)R}{(Y_0 R + 1)\omega L}\right] \tag{4.16}$$

Equation for group delay can be derived by partial differentiation $\angle S_{11}$ and substituting the resonance condition $\omega L = \frac{1}{\omega C}$.

$$\tau_{g,RP}\big|_{\omega=\omega_0} = -\frac{\partial \angle S_{11,RP}}{\partial \omega}\Big|_{\omega=\omega_0} = \frac{4R^2 Y_0 C}{(RY_0)^2 - 1} \tag{4.17}$$

$$S_{11,RP}\big|_{\omega=\omega_0} = \frac{RY_0 - 1}{RY_0 + 1} \tag{4.18}$$

It can be see that when $|RY_0|$ is smaller than 1, i.e., R is smaller than 50 Ohm, the negative group delay would be achieved. The value of the group delay is determined by the resistance and load admittance/impedance, as well as the capacitance/inductance. As $|RY_0|$ approaching to 1, the group delay variation becomes larger as shown in Fig. 4. 13.

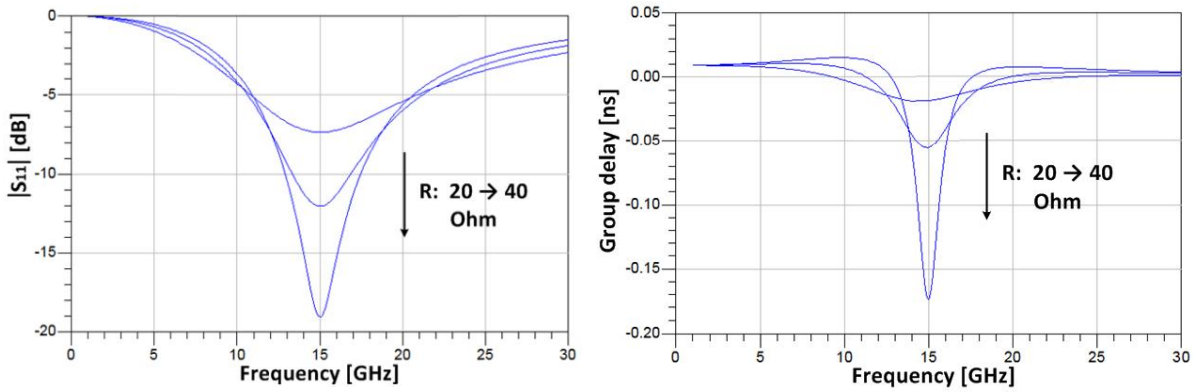

(a) (b)

Fig. 4. 13: (a) The amplitude response of S_{11} and (b) group delay for reflection-type NGD circuits (L=0.23 nH, C=0.49 pF, R=20, 30, 40 Ohm and Z_0=50 Ohm)

The reflection-type NGD (RNGD) circuit has a similar property as that of transmission-type NGD circuits which is shown in Fig. 4. 11, in terms of the amplitude response and group delay variation; the larger group delay variation is accompanied by the larger attenuation. However, comparing them to each other, it can be found that RNGD circuits have a larger bandwidth while smaller group delay variation when the capacitance and inductance are kept as the same for two cases. In next section, the resistance in the RNGD circuit will be replaced by a negative resistance, which would cause an opposite property in the amplitude response.

4.4.2 Reflection-type NGD circuits with negative resistance

Recalling Equation (4.17) and (4.18) , it can be found that if the resistance is negative, $|S_{11,RP}|$ could be more than 1, which means a positive gain is obtained, while the group delay is still negative when the condition $|RY_0| < 1$ is satisfied, i.e., -50 Ohm $< R <$ 0 Ohm when Z_0 is equal to 50 Ohm. The corresponding amplitude

response of S_{11} and group delay with different values of negative resistances are plotted in Fig. 4. 14.

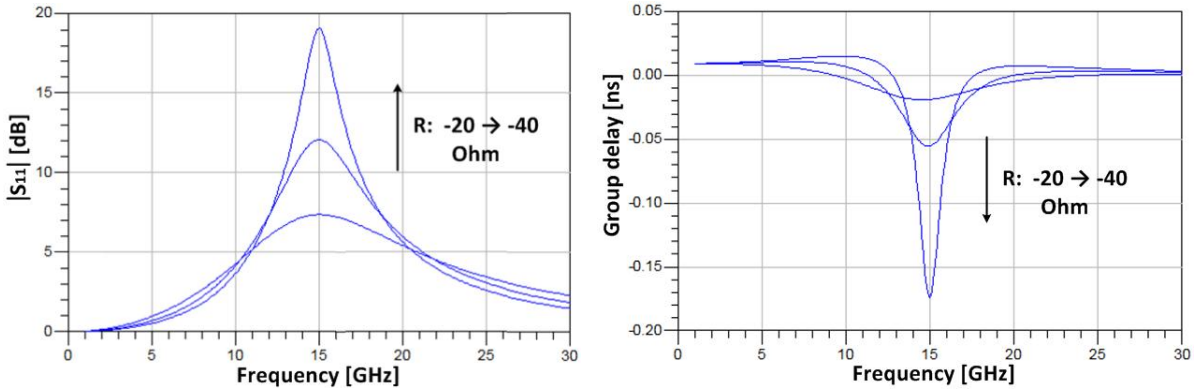

(a) (b)

Fig. 4. 14: (a) The amplitude response of S_{11} and (b) group delay for RNGD circuits with parallel resonator (L=0.23 nH, C=0.49 pF, R=-20, -30, -40 Ohm and Z_0=50 Ohm)

It is obvious that the amplitude response of RNGD circuit with negative resistance shows a convex property which is opposite to the one of previous NGD circuits, while the group delay is still kept to be negative. In the case, the larger group delay variation would be accompanied by larger gain at the resonant frequency. Thus, the RNGD circuit with negative resistance can be used to compensate the attenuation of the conventional NGD circuit. The implementation of negative resistance will be presented in the next section.

In addition, a series LC resonator loaded by negative resistance could also generate the negative group delay as shown in Fig. 4. 15.

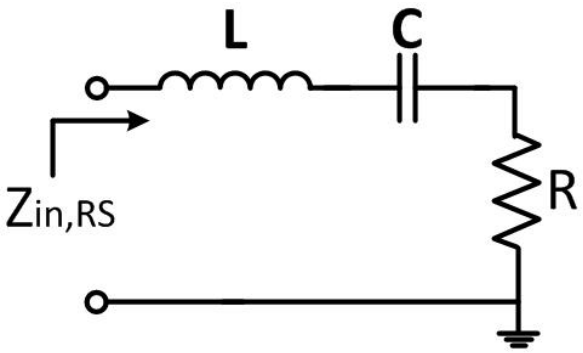

Fig. 4. 15: The reflection-type negative group delay circuit with series resonator

Similar to the case of RNGD with parallel resonator, the reflection coefficient and group delay can be derived as follows.

$$Z_{in,RS} = R + j\omega L + \frac{1}{j\omega C} \tag{4.19}$$

$$S_{11,RS} = \Gamma_{RS} = \frac{Z_{in,RS} - Z_0}{Z_{in,RS} + Z_0}$$

$$= \frac{R - Z_0 + j(\omega L - \frac{1}{\omega C})}{R + Z_0 + j(\omega L - \frac{1}{\omega C})} \tag{4.20}$$

$$\angle S_{11,RS} = tan^{-1}\left[\frac{(\omega^2 LC - 1)}{(R - Z_0)\omega C}\right] - tan^{-1}\left[\frac{(\omega^2 LC - 1)}{(R + Z_0)\omega C}\right] \tag{4.21}$$

$$\tau_{g,RS}\Big|_{\omega=\omega_0} = -\frac{\partial \angle S_{11,RS}}{\partial \omega}\Big|_{\omega=\omega_0} = -\frac{4LZ_0}{(R + Z_0)(R - Z_0)} \tag{4.22}$$

$$S_{11,RS}\Big|_{\omega=\omega_0} = \frac{R - Z_0}{R + Z_0} \tag{4.23}$$

From Equation (4.22), it can be found that when $R < -Z_0$, the negative group delay would be obtained, and the gain shows up “convex”. The typical amplitude response of S_{11} and corresponding group delay are plotted in Fig. 4. 16, as the resistance varies from -20 Ohm to -30 Ohm.

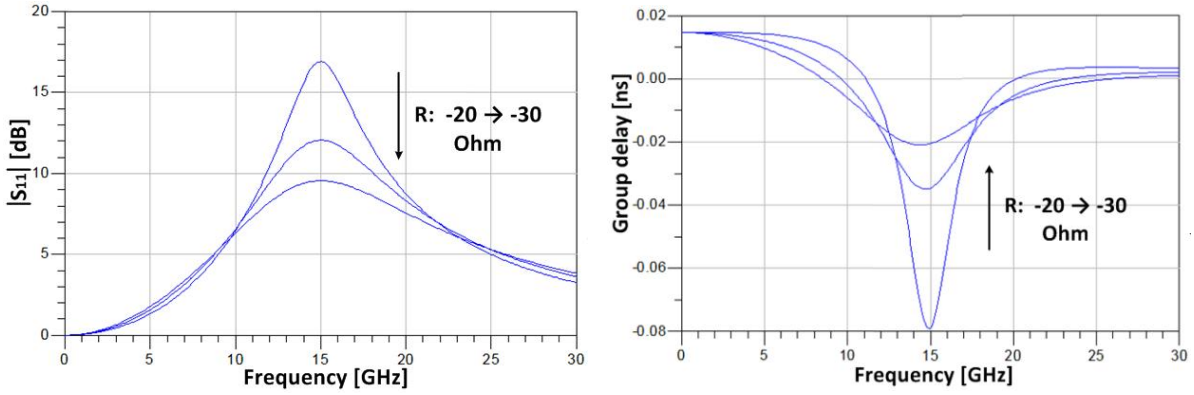

(a) (b)

Fig. 4. 16: (a) The amplitude response of S_{11} and (b) group delay for RNGD circuits with series resonator (L=0.23 nH, C=0.49 pF, R=-20, -25, -30 Ohm and Z_0=15 Ohm)

Note that, here the load impedance Z_0 is chosen to be 15 Ohm. In order to generate NGD, the negative resistance has to be smaller than $-Z_0$. However, for the case with standard load impedance, i.e., 50 Ohm, a negative resistance with value smaller than -50 is difficult to be obtained (since smaller negative resistance means larger gain) while it would be easier when loading the impedance Z_0 of 15 Ohm. From Fig. 4. 16, it can be seen that three negative resistance (-20, -25, -30 Ohm) can all generate negative group delay and when the negative resistance approaches - Z_0, larger group delay variation would be obtained as well as a larger gain. The performance of RNGD circuits is also determined by the capacitor and inductor, since they not only determine the resonance frequency, where a minimum negative group delay would occur, but also determine the quality factor (Q) of the resonator, which would affect the bandwidth and delay time. The rule of thumb shows that the bandwidth is inversely proportional to the minimum value of NGD, i.e., larger group delay variation would cause smaller bandwidth and vice versa.

4.4.3 Negative resistance implementation - Reflection amplifier

The negative resistance can be realized by using a reflection amplifier. If ignoring reflection amplifier's parasitic capacitances, it can be equivalently modeled as a resistor with negative impedance. The circuit of a single-ended reflection amplifier based on a pHEMT transistor is shown in Fig. 4. 17 [43].

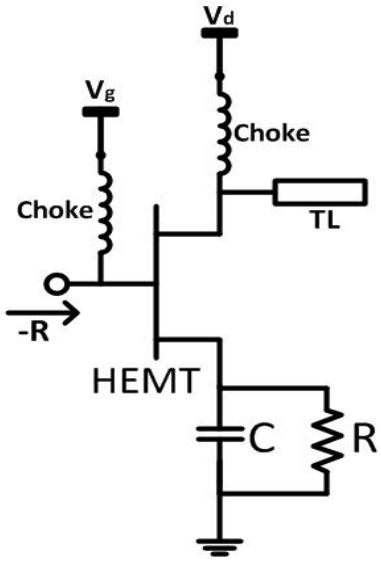

Fig. 4. 17: The schematic of a single-ended reflection amplifier

The gate and drain are biased through inductor ac chokes. The resistor at source is used to limit drain current and control the gate-source bias while the capacitor at the source helps to bring the amplifier into the unstable region [43]. An open-stub transmission line is connected to the drain in order to select the frequency band yielding the negative input resistance at the desired frequency [44].

By choosing appropriate values for the capacitor and the resistance as well as the bias point, the input impedance could be negative. More details about the derivation are described in [45].

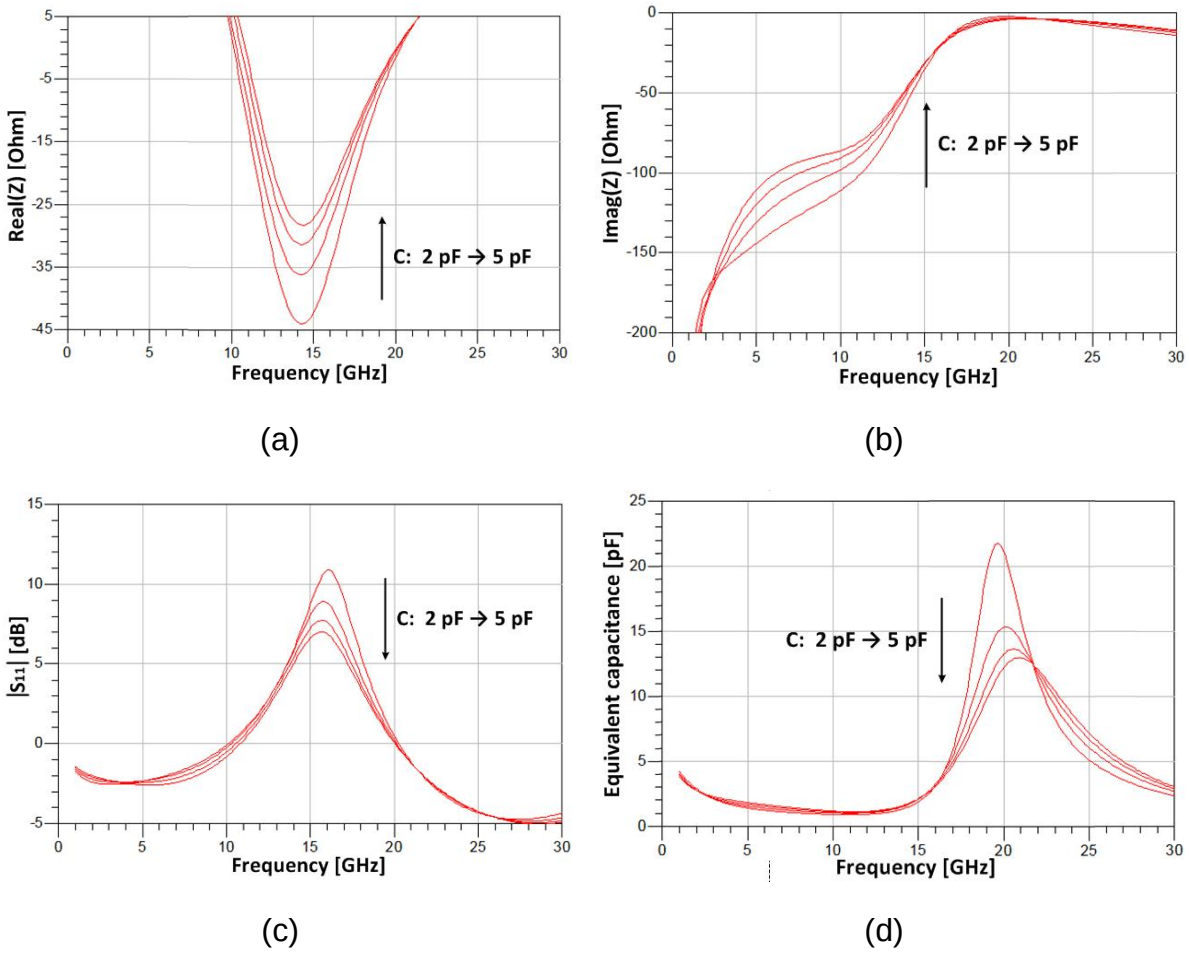

Fig. 4. 18: (a) The equivalent input resistance and (b) the input reactance; (c) the amplitude response of S_{11} and (d) equivalent input parasitic capacitance for the reflection amplifier varied by the capacitor in the source (C = 2, 3, 4, 5 pF).

The equivalent input resistance and reactance of the reflection amplifier varied by the capacitor at the source are shown in Fig. 4. 18(a) and (b), where the gate bias V_g and the drain bias V_d is 0 V and 1 V respectively; the resistance R at the source

is fixed to be 14 Ohm while the capacitor C is varied form 2 pF to 5 pF with the step of 1 pF. Also, Fig. 4. 18(c) and (d) present the amplitude of reflection coefficient of the reflection amplifier and the equivalent input capacitance which is derived from Fig. 4. 18(d).

It can be seen that as the capacitance increases from 2 pF to 5 pF, the maximum value of reflection coefficient decreases from 10.9 dB to 6.8 dB; and the minimum value of the negative resistance changes from -44 to -28 Ohm. The imaginary part of the input impedance (Fig. 4. 18(b)) are all negative throughout all frequencies which means the input impedance of the reflection amplifier can be equivalently modeled as the series of a negative resistor and a parasitic capacitor which is shown in Fig. 4. 18(d). At the frequency of 15 GHz, the value of the equivalent input capacitance is approximately 2 pF for all cases.

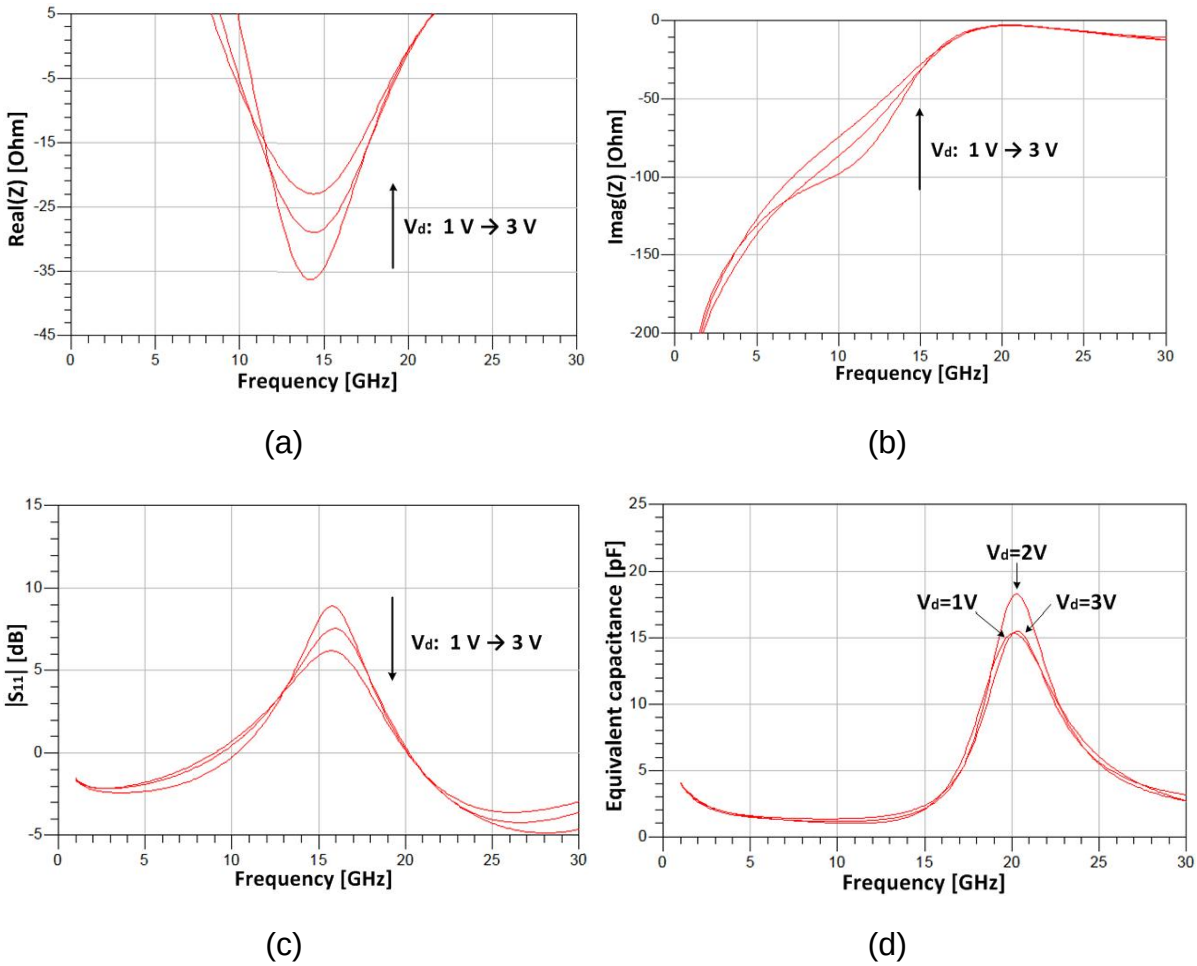

Fig. 4. 19: (a) The equivalent input resistance and (b) the input reactance; (c) the amplitude response of S_{11} and (d) equivalent input parasitic capacitance for the reflection amplifier varied by the drain bias (V_d = 1, 2, 3 V).

In addition, the performance of the reflection amplifier can be varied by the drain bias V_d as shown in Fig. 4. 19, where the gate bias V_g and the resistance R at the source are still 0 V and 14 Ohm respectively; the capacitor C is fixed to 3 pF while V_d is varied form 1 V to 3 V.

As drain bias voltage changes from 1 V to 3V, the maximum value of $|S_{11}|$ decreases from 8.9 dB to 6.1 dB, correspondingly, the minimum value of the negative resistance increases from -36 Ohm to -22 Ohm. The input reactance also shows the capacitive property and the input capacitance achieves 2 pF at 15 GHz for all cases.

Above all, it can be concluded that a reflection amplifier could be implemented as a negative resistance and its performance is determined by the bias point as well as the selection of the lumped components. However, the negative resistance is usually accompanied by a parasitic capacitance, which needs to be taken into the consideration when designing the resonator in the RNGD circuit.

4.4.4 Group delay equalizer based on NGD circuits

As the discussion in the section 4.4.2, the reflection-type negative group delay (RNGD) circuit with negative resistance can be used to compensate the attenuation of the conventional NGD circuits. Due to the reflective character of RNGD circuits, a circulator has to be used to transmit the reflected signal of RNGD into the output (port 2) as shown in Fig. 4. 20. The RNGD circuit consists of a negative resistance (reflection amplifier) and a resonator which could be either parallel or series *L*,*C*, *R* circuit.

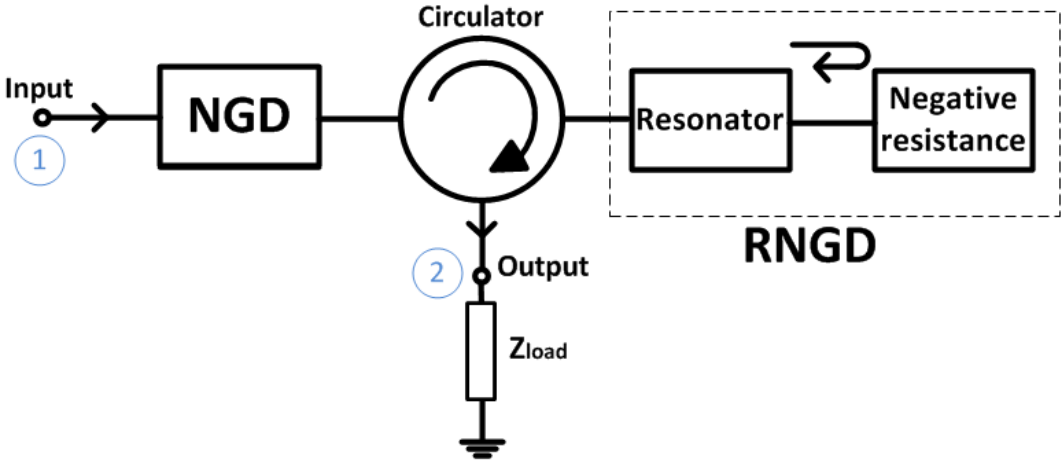

Fig. 4. 20: The topology for group delay equalizer based on NGD circuits

The amplitude response of S_{11} for RNGD circuit with negative resistance as well as the amplitude response of S_{21} for NGD circuit and overall circuit are shown in Fig. 4. 21(a), followed by their group delay response in Fig. 4. 21(b). The circulator's loss is ignored.

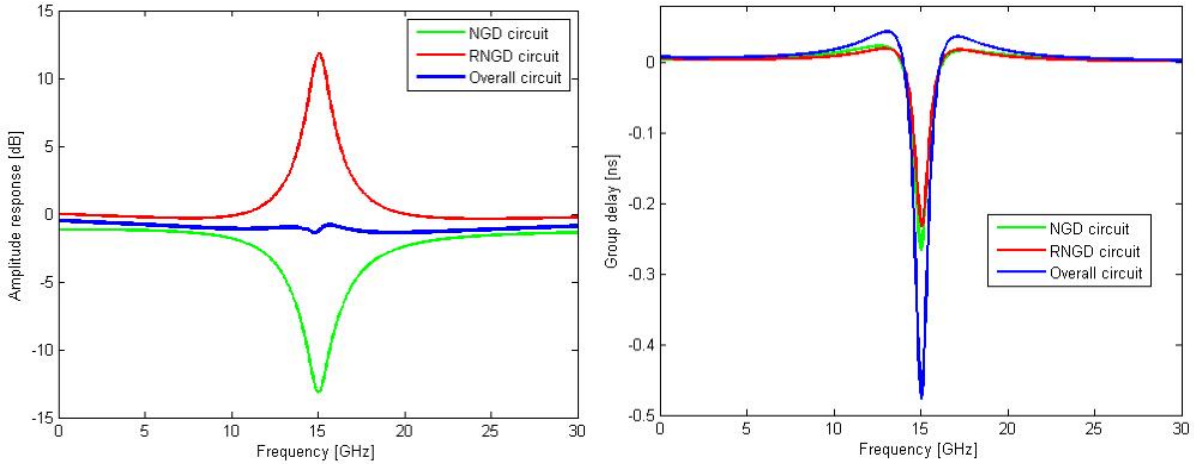

(a) (b)

Fig. 4. 21: (a) The amplitude response of S_{11} for RNGD circuit with negative resistance and S_{21} for NGD circuit and overall circuit; and (b) group delay response of RNGD, NGD and overall circuit

It can be seen that the group delay variation of RNGD circuit with negative resistance is comparable with that of the passive negative group delay circuit. After cascading two circuits, the negative group delay is a sum of that for two circuits. The convex gain in RNGD circuit is utilized to compensate attenuation of the conventional NGD circuit, resulting in an almost flat amplitude response of the overall circuit with the amplitude variation less than 0.6 dB. Thus, the proposed topology demonstrates a quasi all-pass characteristic. Furthermore, the minimum negative group delay time of overall circuit is -0.48 ns, which is a sum of the group delay of a conventional NGD circuit and RNGD circuit. It is almost 2 times of that for a conventional NGD circuit. Therefore, the proposed circuit can be used as a group delay equalizer without affecting the amplitude response.

For example, the proposed NGD equalizer is used to compensate the group delay variation of a low-pass filter, and the results are shown in Fig. 4. 22. It can be found that the group delay variation in the edge of pass band is reduced significantly while the amplitude response is affected only marginally. Within pass band of the low-pass filter, i.e. 0-15GHz, the group delay variation is reduced from 0.6 ns to 0.2 ns; corresponding $|S_{21}|$ reduction is less than 0.53 dB. Similarly, a band-pass filter

has group delay variations in two sides of passband. As a consequence, two NGD equalizers with different resonance frequencies are required to compensate each side of GDVs respectively.

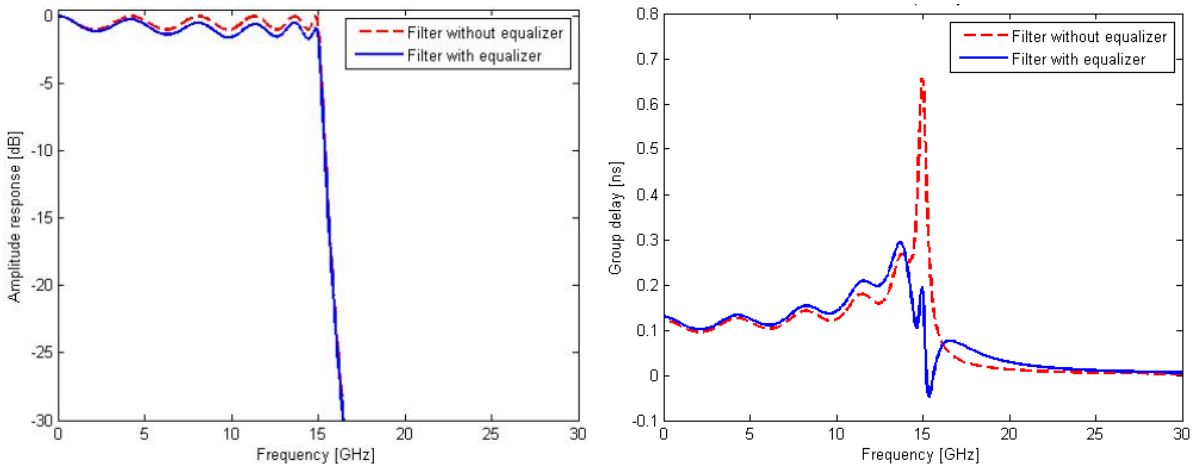

(a) (b)

Fig. 4. 22: (a) The amplitude response and (b) the group delay response of a low-pass filter and a low-pass filter with the equalizer

It is difficult to design circulators in MMIC technology. An alternative approach is to use 90^0 hybrid coupler which is easily implemented in planar technology. An example of a reflection-type negative group delay (RNGD) circuits connected to a hybrid coupler is presented in [42]. In this case, two identical RNGD circuits with negative resistance are needed, as shown in Fig. 4. 23.

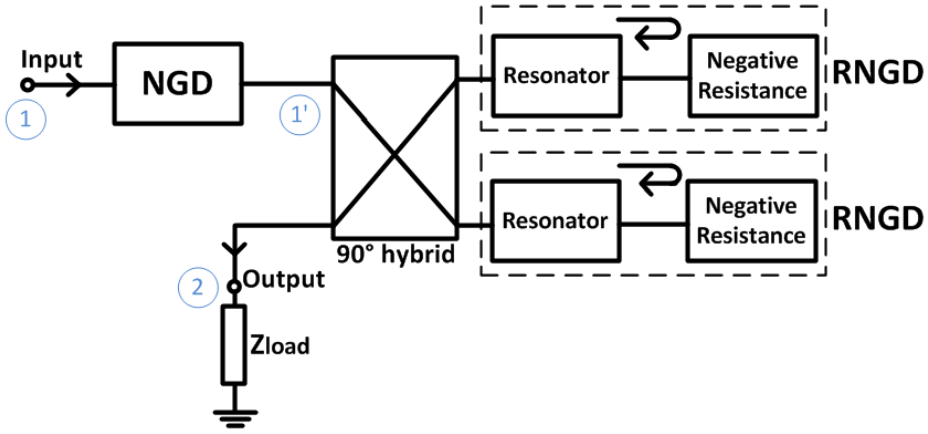

Fig. 4. 23: The alternative topology for group delay equalizer based on NGD circuits

Due to the property of the 90^0 hybrid coupler, two reflected signal would cancel each other in the input (port 1') while sum up together in the output (port 2). The 90^0 hybrid coupler [46] is implemented as shown in Fig. 4. 24 and the simulation result is shown in Fig. 4. 25.

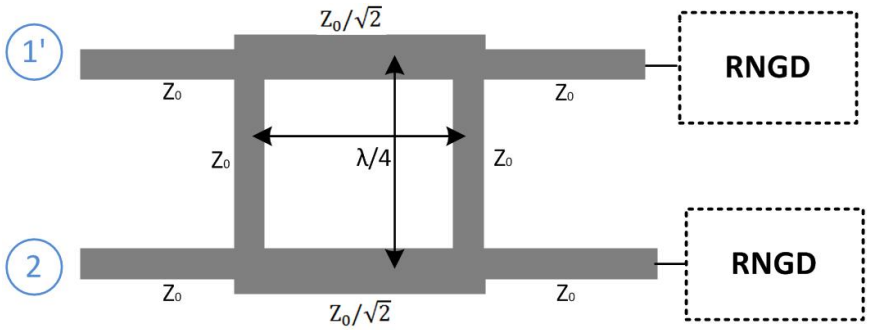

Fig. 4. 24: The quadrature (90^0) hybrid coupler with two identical RNGD circuits

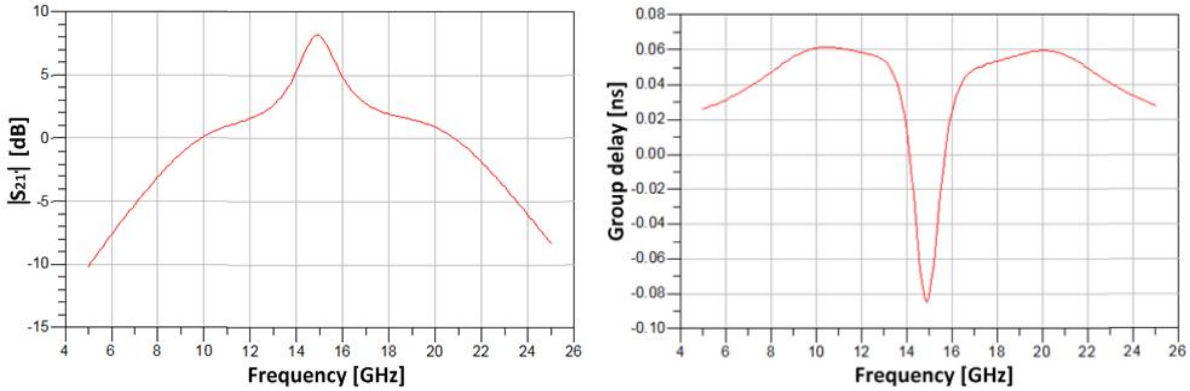

(a) (b)

Fig. 4. 25: (a) The amplitude response of $S_{21'}$ and (b) the group delay response corresponding to the topology in Fig. 4. 24

It can be seen that the reflected signal of RNGD circuits is transmitted to the output port (Port 2). Cascading the hybrid with conventional NGD circuits as shown in Fig. 4. 23, the total amplitude response and the group delay response is presented in Fig. 4. 26.

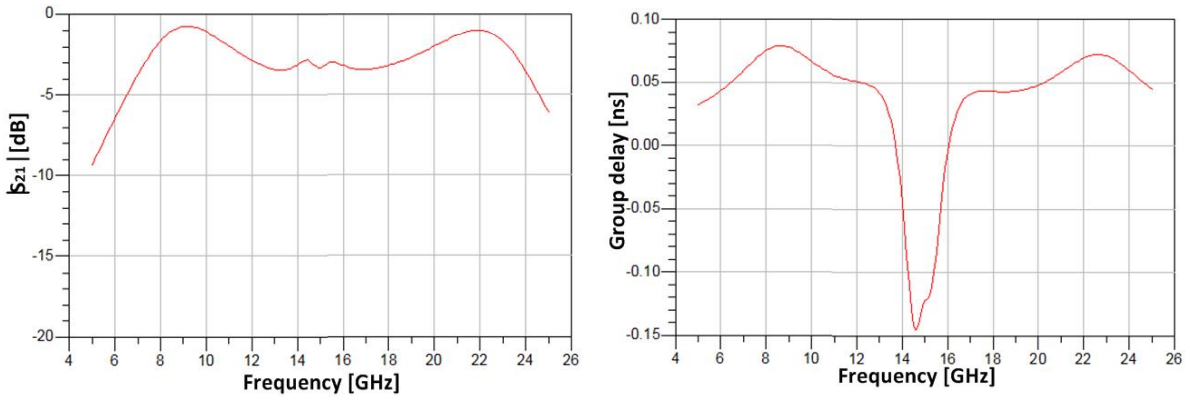

(a) (b)

Fig. 4. 26: (a) The amplitude response of S_{21} and (b) the group delay response corresponding to the topology in Fig. 4. 24

It can be seen that the negative group delay is achieved with the minimum value of -0.15 ns, while the total amplitude response is kept as almost flat between 11 GHz an 19 GHz (amplitude variation is smaller than 1dB). Thus, the proposed planar topology can be used for group delay equalization. However, its operation bandwidth is limited by the bandwidth of the 90^0 hybrid coupler, since the quarter-wave length is required in the hybrid coupler. In order to increase the bandwidth, the hybrid with multiple sections can be used.

Chapter 5

Conclusions and future work

Several microwave components can introduce group delay variation, which would distort the signal and degrade the system performance. A band-pass filter is one example, which creates a group delay variation near the edge of pass band, i.e., in transition areas of filters. According to simulations of ideal filter components (Q is infinite) in ADS, it shows that the Elliptic band-pass filter has the largest group delay variation compared with other types of filters (with same order), e.g., Chebyshev, Butterworth and Bessel-Thomson filters. For example, a 5th-order Elliptic band-pass filter with stopband rejection of 20 dB and pass-band frequency from 7.5 GHz to 12.5 GHz would introduce a maximum group delay variation of 3.4 ns, while a Chebyshev band-pass filter with the same parameters would only introduce group delay variation of 1.1 ns. However, the Elliptic band-pass filter has the steepest slope amplitude response at the edge the pass-band.

With the help of *MATLAB*, effects of group delay variations from band-pass filters for 4QAM and 16QAM modulation are investigated in terms of the bit error rate and penalty power. In the simulations, group delay variation is added in the receiver front end, while other components in the transceiver are assumed to be perfect. The results show that group delay variation with the peak of 3.4 ns, which is introduced by the 5th-order Elliptic band-pass filter, would cost extra power of 0.8 dB and 1.6 dB for 4QAM and 16QAM modulation respectively, in order to achieve the same performance (BER = 10^{-4}) as the system without any group delay variation. In contrast, the Bessel-Thomson filter has smallest group delay variations and costs almost 0 dB penalty power to achieve the same performance. Based on simulation results, it can be inferred that for systems using high-order modulation with high power spectral efficiency, such as 64QAM or 256QAM, the group delay variation would cause the penalty power with several dB, so that the effect of group delay variations need to be taken into consideration and group delay equalizers are necessitated.

Also, analog group delay equalizers are investigated, which are realized based on two methodologies: 1) all-pass networks; 2) negative group delay circuits. Second-

order all-pass networks based on lumped and distributed elements are implemented. The simulation result shows that an all-pass network with distributed elements has a larger bandwidth while a smaller group delay variation comparing with its lumped elements counterpart. However, the performance of both networks is limited by the quality factor (Q) of elements; smaller Q values would cause larger attenuation at the frequency where the maximum group delay occurs. The ''convex'' group delay of all-pass networks can be used to compensate ''concave'' group delay of band-pass filters, but unavoidably the total group delay time of the system will increase.

In contrast, a negative group delay circuit is able to suppress the group delay increasing in transition areas of filters without increasing the total group delay time. Unfortunately, a negative group delay circuit suffers a large attenuation, e.g., 8 dB loss to achieve group delay with the value of -0.09 ns at 15GHz. In this work, a novel group delay equalizer circuit topology is proposed to reduce the attenuation, which consists of a reflection-type negative group delay circuit with negative resistance and a circulator, as well as a traditional NGD circuit. The proposed equalizer has a flat amplitude response with a variation less than 0.6 dB, keeping a feature of negative group delay. For example, the proposed equalizer is used to compensate the group delay variation from a low-pass filter with passband from DC to 15 GHz. The simulation result presents that the group delay variation of the filter is reduced from 0.6 ns to 0.2 ns while the amplitude response is reduced less than 0.53 dB. Those results demonstrate that the proposed group delay equalizer has potential to be applied in microwave communication systems.

Future work can be divided into two parts. First, effects of group delay variation on communication systems need to be analyzed and investigated more systematically, for instance, in the case of higher-order modulation format signals, such as 1024 QAM. Furthermore, it is necessary to investigate the effect of different types of group delay variations, such as linear, rippled and higher-order group delay variations.

Second, the proposed equalization topology needs to be validated by experiments. Since the load impedance highly affects the performance of the negative group delay circuit, the impedance matching networks might be included in the reality circuit. Furthermore, the proposed RNGD circuit with negative resistance can be used individually as a NGD generator with gain. More applications related to the proposed NGD generator need to be investigated further.

Bibliography

[1] Roberto Aiello and Anui Batra, *Ultra wideband systems: technologies and applications*. Boston: Newnes, 2006.

[2] Xinping Huang and M. Caron, "Type-Based Group Delay Equalization Technique," *Circuits and Systems I: Regular Papers, IEEE Transactions on*, vol. 58, no. 7, pp. 1661 - 1670, July 2011.

[3] S. Gupta et al., "Group-Delay Engineered Noncommensurate Transmission Line All-Pass Network for Analog Signal Processing," *Microwave Theory and Techniques, IEEE Transactions on*, vol. 58, no. 9, pp. 2392 - 2407, Sep. 2010.

[4] E.G. Cristal, "Theory and Design of Transmission Line All-Pass Equalizers," *Microwave Theory and Techniques, IEEE Transactions on*, vol. 17, no. 1, pp. 28 - 38, Jan 1969.

[5] Herman J. Blinchikoff and Anatol I. Zverev, *Filtering in the Time and Frequency Domains*. New York: Wiley, 1976.

[6] S. Abielmona, S. Gupta, and C. Caloz, "Compressive Receiver Using a CRLH-Based Dispersive Delay Line for Analog Signal Processing," *Microwave Theory and Techniques, IEEE Transactions on*, vol. 57, no. 11, pp. 2617 - 2626, Nov. 2009.

[7] V.S. Dolat and R.C. Williamson, "A Continuously Variable Delay-Line System," *1976 Ultrasonics Symposium* , pp. 419 - 423, 1976.

[8] W.S. Ishak, "Magnetostatic wave technology: a review," *Proceedings of the IEEE*, vol. 76, no. 2, pp. 171 - 187, 1998.

[9] J.D. Adam, M.R. Daniel, and C.E. Nothnick, "MSW Dispersive Delay Lines in a Compressive Receiver," *1982 Ultrasonics Symposium* , pp. 533 - 536, 1982.

[10] M.A.G. Laso et al., "Chirped delay lines in microstrip technology," *Microwave and Wireless Components Letters, IEEE*, vol. 11, no. 12, pp. 486 - 488, 2001.

[11] L. Ranzani et al., "Microwave-Domain Analog Predistortion Based on Chirped Delay Lines for Dispersion Compensation of 10-Gb/s Optical Communication Signals," *Lightwave Technology*, vol. 26, no. 18, pp. 2641 - 2646, 2008.

[12] M. Coulombe and C. Caloz, "Reflection-Type Artificial Dielectric Substrate Microstrip Dispersive Delay Line (DDL) for Analog Signal Processing," *Microwave Theory and Techniques, IEEE Transactions on* , vol. 57, no. 7, pp. 1714 - 1723 , July 2009.

[13] Christophe Caloz and Tatsuo Itoh, *Electromagnetic Metamaterials: Transmission Line Theory and Microwave Applications*. NY: Wiley, 2005.

[14] K. Murase, R. Ishikawa, and K. Honjo, "Group delay equalised monolithic microwave integrated circuit amplifier for ultra-wideband based on right/left-handed transmission line design approach," *Microwaves, Antennas & Propagation, IET* , vol. 3, no. 6, pp. 967 - 973, Sep. 2009.

[15] S. Abielmona, S. Gupta, and C. Caloz, "Experimental Demonstration and Characterization of a Tunable CRLH Delay Line System for Impulse/Continuous Wave," *Microwave and Wireless Components Letters, IEEE* , vol. 17, no. 12, pp. 864 - 866, Dec. 2007.

[16] S. Lucyszyn, I.D. Robertson, and A.H. Aghvami, "Negative group delay synthesiser," *Electronics Letters* , vol. 29, no. 9, pp. 798 - 800, April 1993.

[17] Kyoung-Pyo Ahn, R. Ishikawa, and K. Honjo, "Low Noise Group Delay Equalization Technique for UWB InGaP/GaAs HBT LNA," *Microwave and Wireless Components Letters*, vol. 20, no. 7, pp. 405 - 407, July 2010.

[18] Kyoung-Pyo Ahn, R. Ishikawa, and K. Honjo, "Group Delay Equalized UWB InGaP/GaAs HBT MMIC Amplifier Using Negative Group Delay Circuits," *Microwave Theory and Techniques, IEEE Transactions on*, vol. 57, no. 9, pp. 2139 - 2147 , Sep. 2009.

[19] B. Ravelo, A. Perennec, and M. Le Roy, "Equalization of interconnect propagation delay with negative group delay active circuits," in *Signal Propagation on Interconnects, 2007. SPI 2007. IEEE Workshop on* , 2007, pp. 15 - 18.

[20] Govind P. Agrawal, *Lightwave technology : telecommunication systems*. N.J.: Wiley, 2005.

[21] http://www.rp-photonics.com/dispersion_shifted_fibers.html.

[22] Donald J. Lanzinger, "Group Delay Caused by Impedance Mismatch," in *ARFTG Conference Digest-Spring, 29th*, 1987, pp. 247-264.

[23] A.R. EskandariL and L. Mohammadi, "Group Delay Variations in Wideband Transmission Lines: Analysis and Improvement," *International Journal of Soft Computing & Engineering*, vol. 1, no. 4, 2011.

[24] J. G. Proakis, *Digital Communications*.: McGraw-Hill Higher Education, 2007.

[25] Andrea Goldsmith, *Wireless Communications*.: Cambridge University Press, 2005.

[26] Arthur Bernard Williams and Fred J. Taylor, *Electronic Filter Design Handbook, Fourth Edition*.: McGraw-Hill , 2006.

[27] S. J. Erickson, "An analysis of negative group delay in electronic circuits," University of Toronto (Canada), ProQuest Dissertations and Theses 2005.

[28] M. Kitano, "Negative group delay and superluminal propagation: an electronic circuit approach," *Selected Topics in Quantum Electronics, IEEE Journal of*, vol. 9, no. 1, pp. 43 - 51 , Feb. 2003.

[29] Morgan W. Mitchell and Raymond Y. Chiao, "Causality and negative group delays in a simple bandpass amplifier," *American Journal of Physics*, vol. 66, no. 1, pp. 14-19, 1998.

[30] Daniel Solli, R. Y. Chiao, and J. M. Hickmann, "Superluminal effects and negative group delays in electronics, and their applications," *Physical review. E, Statistical, nonlinear, and soft matter physics*, vol. 66, pp. 056601.1-056601.4, 2002.

[31] John R. Barry, Edvard A. Lee, and David G. Messerschmitt, *Digital communication*. Boston: Kluwer Academic, 2004.

[32] A. Azizzadeh, "Degradation of BER by Group Delay in Digital Phase Modulation," in *The Fourth Advanced International Conference on Telecommunications*, 2008, pp. 350-354.

[33] http://en.wikipedia.org/wiki/Additive_white_Gaussian_noise.

[34] R. Levy, "Realization of Practical Lumped Element All-Pass Networks for Delay Equalization of RF and Microwave Filters," *Microwave Theory and Techniques, IEEE Transactions on*, vol. 59, no. 12, pp. 3307-3311, Dec. 2011.

[35] R. Ishikawa and K. Honjo, "Group delay equalised monolithic microwave integrated circuit amplifier for ultra-wideband based on right/left-handed transmission line design approach," *Microwaves, Antennas & Propagation, IET*, pp. 967-973, September 2009.

[36] E.G. Cristal, "Analysis and Exact Synthesis of Cascaded Commensurate Transmission-Line C-Section All-Pass Networks," *Microwave Theory and Techniques, IEEE Transactions on*, vol. 14, no. 6, pp. 285 - 291, June 1966.

[37] Y. Horii, S. Gupta, B. Nikfal, and C. Caloz, "Multilayer Broad-Coupled Dispersive Delay Structures for Analog Signal Processing," *IEEE Microwave and Wireless Components Letters*, vol. 22, no. 1, Jan. 2012.

[38] C.D. Broomfield, "Broadband negative group delay networks for compensation of microwave oscillators and filters," *Electronics Letters*, vol. 36, no. 23, pp. 1931 - 1933 , Nov. 2000.

[39] Heungjae Choi, Kyungju Song, Chul Dong Kim, and Yongchae Jeong, "Synthesis of negative group delay time circuit," in *Microwave Conference, 2008. APMC 2008. Asia-Pacific*, 2008, pp. 1 - 4.

[40] B. Ravelo, A. Perennec, M. Le Roy, and Y.G. Boucher, "Active Microwave Circuit With Negative Group Delay," *Microwave and Wireless Components Letters, IEEE*, vol. 17, no. 12, pp. 861 - 863, Dec. 2007.

[41] Symon K. Podilchak, Brian M. Frank, Al P. Freundorfer, and Yahia M. M. Antar, "High speed metamaterial-inspired negative group delay circuits in CMOS for delay equalization," in *Microsystems and Nanoelectronics Research Conference, 2009. MNRC 2009. 2nd*, pp. 9 - 12.

[42] Heungjae Choi, Younggyu Kim, Yongchae Jeong, and Chul Dong Kim, "Synthesis of reflection type negative group delay circuit using transmission line resonator," in *Microwave Conference, 2009. EuMC 2009. European*, 2009, pp. 902 - 905.

[43] H. I. Cantu, "A 21 GHZ Reflection Amplifier MMIC for Retro-Directive Antenna and RFID Applications," in *MM-Wave Products and Technologies*, 2006, pp.

66 - 70.

[44] H.I. Cantu, V.F. Fusco, and S. Simms, "Microwave reflection amplifier for detection and tagging applications," in *Microwaves, Antennas & Propagation, IET*, 2008, pp. 115 - 119.

[45] Metin Yazgi, Ali Toker, and Bal S. Virdee, "A new negative resistance circuit and an application for loss compensation in a distributed amplifier," *ANALOG INTEGRATED CIRCUITS AND SIGNAL PROCESSING*, vol. 60, no. 3, pp. 215 - 220, 2009.

[46] David M. Pozar, *Microwave engineering*. Hoboken, NJ: Wiley, 2004.